Western Norway University of Applied Sciences

BACHELOR'S THESIS

Modelling the effect of surface hoar formation on the temperature gradient and vapor pressure gradient in a snowpack

Modellering av effekten av overflaterimdannelse på temperatur- og damptrykkgradienten i et snødekke

Just Cristian Lundberg, Brage Storebakken and Natalia Zieritz

Geology and Geohazards
Department of Environmental Sciences
Supervisor: Simon de Villiers
03.06.2019

We confirm that the work is self-prepared and that references/source references to all sources used in the work are provided, cf. Regulation relating to academic studies and examinations at the Western Norway University of Applied Sciences (HVL), § 10.

Preface

This thesis marks the end of a bachelor's degree in Geology and Geohazards at Western Norway University of Applied Sciences (HVL).

We would like to thank our supervisor Simon de Villiers, whose early morning thinking sessions inspired this thesis. Thank you for all help and your everlasting optimism. Thanks to HVL for lending us the weather station, and to the library for tracking down articles that were difficult to find. The data provided from the Norwegian Water Resources and Energy Directorate (NVE) and technical support on the weather station from the Geological Survey of Denmark and Greenland (GEUS) is greatly appreciated. Last but not least, we want to thank field- and therapy dog Topper for emotional support.

Sogndal, 3. Juni 2019

Just Cristian Lundberg Brage Storebakken Natalia Zieritz

Abstract

Buried surface hoar layers and faceted crystals are both typical persistent weak layers for initiating an avalanche. Faceted crystals are formed under large vapor pressure gradients which are made by large temperature gradients. This paper discusses what effect the latent heat release from surface hoar growth has on the temperature gradients and corresponding vapor pressure gradients in the snowpack. This was investigated using an automatic weather station placed at Hollekvebrui in Sogndalsdalen, Norway, and measuring the surface hoar formed during a night through mass change of the top 10 cm of snow at the same location. The data gathered was used to develop a numerical simulation that solves the heat equation in one dimension using the finite difference method. The model was developed in several steps that each were modified to calibrate it to more realistic levels. In the final model data inputs from the weather station and mass difference were implemented, and the model shows that a mass gain of 0.094 kg has little effect on the temperature and vapor pressure gradients in the snowpack. However, problems have been found with some of the assumptions that were made around heat transfer in and out of the snowpack, and extending the currently inadequate dataset is necessary to test the findings in this paper.

Sammendrag

Kantkorn og begravde lag av overflaterim er begge typiske vedvarende svake lag som kan føre til snøskred. Kantkorn blir dannet under store damptrykkgradienter som forekommer ved store temperaturgradienter. Denne oppgaven diskuterer hvilken effekt latent varme frigjort fra overflaterimdannelse har på temperaturgradienten og den tilhørende damptrykkgradienten i snødekket. Feltarbeidet ble utført ved Hollekvebrui i Sogndalsdalen, Norge, hvor overflaterim ble målt ved å veie de øverste 10 cm av snøen før og etter en natt med rimdannelse. Data fra feltarbeidet og fra en automatisk værstasjon ble brukt i en numerisk modell, hvor vi bruker endelig differensmetoden for å løse varmeligningen i én dimensjon. Denne modellen ble utviklet stegvis, fra en simpel etterligning til en mer realistisk representasjon av et reelt snølag. Den siste modellen brukte data fra feltarbeid og værstasjonen, og viser at rimdannelse på 0.094 kg har liten effekt på temperatur- og damptrykkgradienten. Noen problemer vedrørende antagelser som er tatt angående varmeoverføring til og fra snøoverflaten, i tillegg til mangelfullt datagrunnlag, gjør at videre undersøkelser er nødvendig for å kunne komme med en endelig konklusjon på temaet.

Table of contents

1. Introduction

Avalanches are a geohazard that can have consequences for infrastructure, as well as for backcountry recreationalists. A lack of avalanche mitigation measures could impact the economy, as roads and buildings can get buried or destroyed. An aspect of these mitigation measures is avalanche forecasting that can predict size, likelihood and the time of arrival of an avalanche. There are two main types of avalanches. Loose snow avalanches are the smallest and they seldom cause damage to people or infrastructure. The other main type, slab avalanches, can be much larger and it is this type that most often result in fatalities and destruction of roads and buildings. To create a slab avalanche, certain factors must be in place. One of these factors is a weak layer and/or a weak interface. Faceted crystals and surface hoar are two types of weak layers that cause avalanches. A study in South-west Montana, USA, found that 31 % of large backcountry avalanches (size three or larger) are caused by a buried layer of surface hoar while 59 % of avalanches are caused by a layer of faceted crystals (Birkeland, Johnson, & Schmidt, 1998). Understanding more about the formation of these weak layers is important. Surface hoar is created during clear nights with high relative humidity and colder temperatures (Stössel, Guala, Fierz, Manes, & Lehning, 2010). The formation of surface hoar provides additional heat into the system due to the condensation of water vapor onto the snow surface from the locally surrounding supersaturated humid air (Stössel et al., 2010). Therefore, the formation of surface hoar will theoretically make the surface temperature higher than what would be expected if only the sensible and radiated heat exchange is considered. If this additional heat was not created, the surface temperature could possibly be lower. Lower surface temperatures result in higher temperature gradients within the snowpack and may contribute to suitable conditions for growth of faceted crystals.

The objective of this bachelor thesis is to explore how the formation of surface hoar affects the temperature gradient and corresponding vapor pressure gradient in the snowpack, and if a lack of surface hoar could lead to a higher likelihood of formation of near surface faceted crystals. This was investigated by making a numerical simulation of the temperature gradient in the snowpack, which made it possible to study how the temperature gradient in the snowpack changes with time. The simulation was made using a finite difference method to solve the heat equation in one dimension. In order to validate the numerical simulation, real data input values were collected during field experiments. Different approaches have been used to find the input values. For the field work, a method described by Stössel et al. (2010) which involved measuring how much surface hoar was created during clear nights, was used. This was done

through measurements of mass changes at the surface of the snow as well as measurements of surface hoar size. Another factor that was considered was the sensible heat provided to the system, calculated from measured wind speeds from an automatic weather station (AWS) at the study site. Colbeck (1988) found that some wind is needed to create surface hoar but did not specify required wind speed, in contrast to the assumptions made by Lang, Leo, & Brown (1984), that surface hoar is only made through vapor diffusion. Further studies on this were done by Hachikubo & Akitaya (1997), who found more exact values for wind speeds needed for surface hoar growth. Based on this, Hachikubo (2001) came up with equations to calculate the sensible heat release based on wind speed. Hachikubo mentions that latent heat release does contribute to the surface energy balance to an extent that is not negligible. To make the parameters relevant for conditions in Norway, we have conducted field work in Sogndalsdalen. The field work included collecting data from a weather station and measuring mass change in the top-layer of the snowpack (accumulation of surface hoar), as well as measuring the temperature in the top of the snowpack and the surrounding weather conditions (longwave and shortwave radiation, humidity and surface temperatures). Ultimately, using these approaches, the aim is to get the most realistic impression on how the temperature in the snowpack changes with time and if surface hoar growth has a significant effect on this temperature.

2. Background

2.1 Heat transfer to and within the snowpack

When modelling temperature change in a snowpack it is important to understand all aspects of heat transfer to, from and within the snow. When computing the energy flux out of the surface of the snowpack using an upper boundary condition, latent, sensible, advective and radiative heat can affect the flux. The computed upper boundary condition includes all terms of the energy balance equation (EQ. 1) except for heat transfer by mass change (not relevant for our study) and heat transfer from the ground, which is modelled in the lower boundary condition. In the model, a thermal diffusivity determines the rate of energy transfer. An understanding of heat transfer between snow grains is needed to find the right diffusivity for our model.

Several articles and books are written on energy exchange and balance in a snowpack, and most of the groundwork was done mid-1900's. The first application of energy transfer theory on a snowpack was done by Sverdrup after his investigations in Western Spitsbergen in 1934 (Anderson, 1976; Sverdrup, 1935). Sverdrup's paper was mainly on turbulent heat transfer, but he also included a full energy balance calculation.

The formula for energy balance at the snow surface may be written as:

$$\Delta Q = Q_n + Q_h + Q_e + Q_g + Q_m \quad (1)$$

Where: Q_n = net radiation transfer

Q_h = sensible heat transfer

Q_e = latent heat transfer

Q_g = heat transfer across the snow-soil interface

Q_m= heat transfer by mass changes (advected heat)

A negative ΔQ will lead to a cooling of the snowpack, and a positive ΔQ will heat it.

Net radiation transfer, also called radiant energy flux, consists of incoming and outgoing shortwave and longwave radiation. Shortwave radiation is electromagnetic radiation in the wavelengths of near-ultraviolet, visible light, and near-infrared (0.1 μm – 4.0 μm). The main source of shortwave radiation is the sun and is thus only affecting the snowpack in daytime. Since snow has an albedo of 0.80-0.97 most of the shortwave radiation is reflected (Brandt & Warren, 1993; Oke, 1995). Albedo can be calculated by dividing incoming shortwave radiation by outgoing shortwave radiation. Due to different albedo for different wavelengths, most of the

absorbed radiation is in the near infrared spectrum (Warren, 1982). Brandt & Warren (1993) used a spectral model where they separated different wavelengths and found that over half of the energy absorbed in the snowpack was absorbed in the top 2 millimeters (figure 1). However, this may vary from site to site because the light transmission varies over time, and because of various optical properties of snow (Järvinen & Leppäranta, 2013). About 1% of the shortwave radiation that has penetrated the surface reaches as deep as 1 meter, due to scattering and absorption (Brandt & Warren, 1993; Warren, 1982).

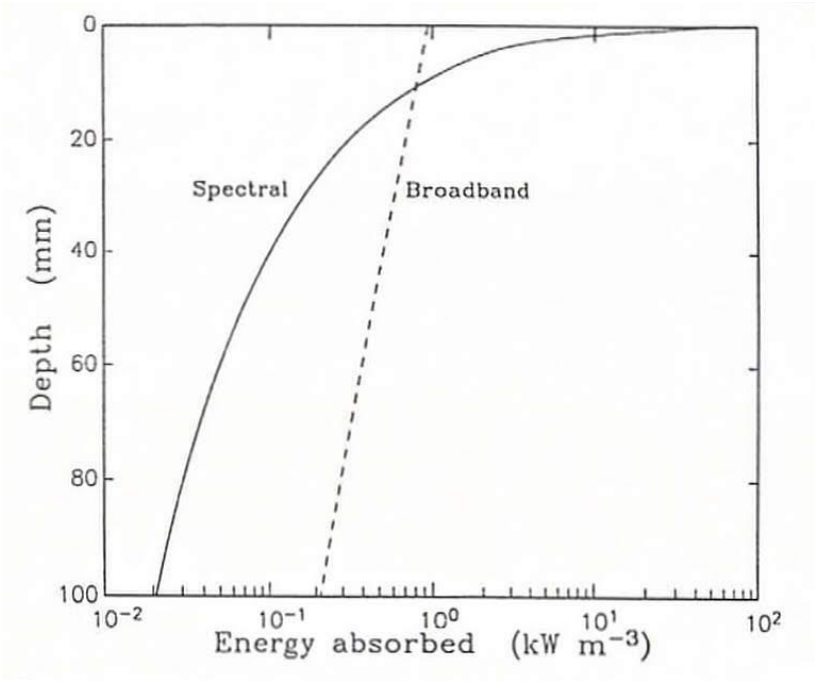

Figure 1: Solar energy absorbed per unit volume (heating rate) as a function of depth in the top 10 cm of the snow, comparing Schlatter's broad-band model with Brandt and Warren's spectral model. The incident solar flux is 400 W/m^2, appropriate for the Antarctic Plateau in December. (Brandt & Warren, 1993).

Longwave radiation, or far-infrared radiation, has a wavelength of 4.0 µm to 120 µm, and predominantly originates from earth's (terrestrial) surface or the atmosphere. The most important source of incoming longwave radiation is clouds.

Outgoing longwave radiative flux φ is calculated using the Stefan-Boltzmann law:

$$\varphi = \varepsilon \, \sigma \, T^4 \qquad (2)$$

where ε, σ and T are emissivity, Stefan-Boltzmann's constant and temperature in Kelvin, respectively. Several articles have studied the longwave radiance from snow and have found snow to closely resemble a perfect blackbody (Oke, 1995; van As, 2011). For all grain sizes emissivity lies between 0.985 – 0.990 (Dozier & Warren, 1982). On clear nights, when there is little incoming longwave radiation, the snow surface can become 20 degrees colder than the air

temperature due to outgoing longwave radiation (Stössel, 2007). It must be emphasized that heat transfer to and from the snowpack due to longwave radiation only occurs at the surface of the snowpack, unlike shortwave radiation, which penetrates further down. This is potentially an important aspect to consider when designing a numerical model for the evolution of temperature gradients.

The net radiation tends to have the largest contribution to the energy balance equation (EQ. 1), with up to 70% of total heating during 24 hours in some cases (Holmgren, 1971).

Sensible heat transfer is part of the turbulent heat exchange at the snow surface, often induced by wind. The name 'sensible' arrives from the idea of the energy being felt with senses. Sensible heat is associated with a change in temperature and includes conduction and convection. Conduction is direct heat transfer from molecule to molecule, and the thermal conductivity is a material's ability to conduct heat. Since the thermal conductivity of air is about four times lower than the conductivity of snow, the thermal effect of conduction from air to snow alone often only has a small effect on the total heat transfer when there is no air transport (McClung & Schaerer, 2006).
Convection is the movement of heat through bulk motion of a substance, which involves the process of both conduction and advection. The snow surface can receive heat when warmer turbulent wind eddies are directed towards the surface (Anderson, 1976; Stössel, 2007; Sverdrup, 1935). In 1971 Holmgren (1971) found that highest sensible heat fluxes occur during nights of high wind velocities and advection of warm and humid air (Holmgren, 1971). He found that the relative importance of sensible heat halved when conditions with clear skies and low winds were present (from 46% to 22%).

Latent heat transfer, also called phase transition heat transfer, is the energy added or removed when changing matter from one state to another. This includes the processes of melting, freezing, evaporation, condensation, sublimation, and deposition (see figure 2). For this project, latent heat transfer is relevant because the deposition of water vapor onto the snow surface releases heat. At 0°C the latent heat released is $2.834*10^6$ J/kg. If this transition happens at colder temperatures, the energy released is lower. The latent heat is assumed to be predominantly absorbed by the snowpack due to its relatively high specific heat capacity and thermal conduction properties in contrast to air.

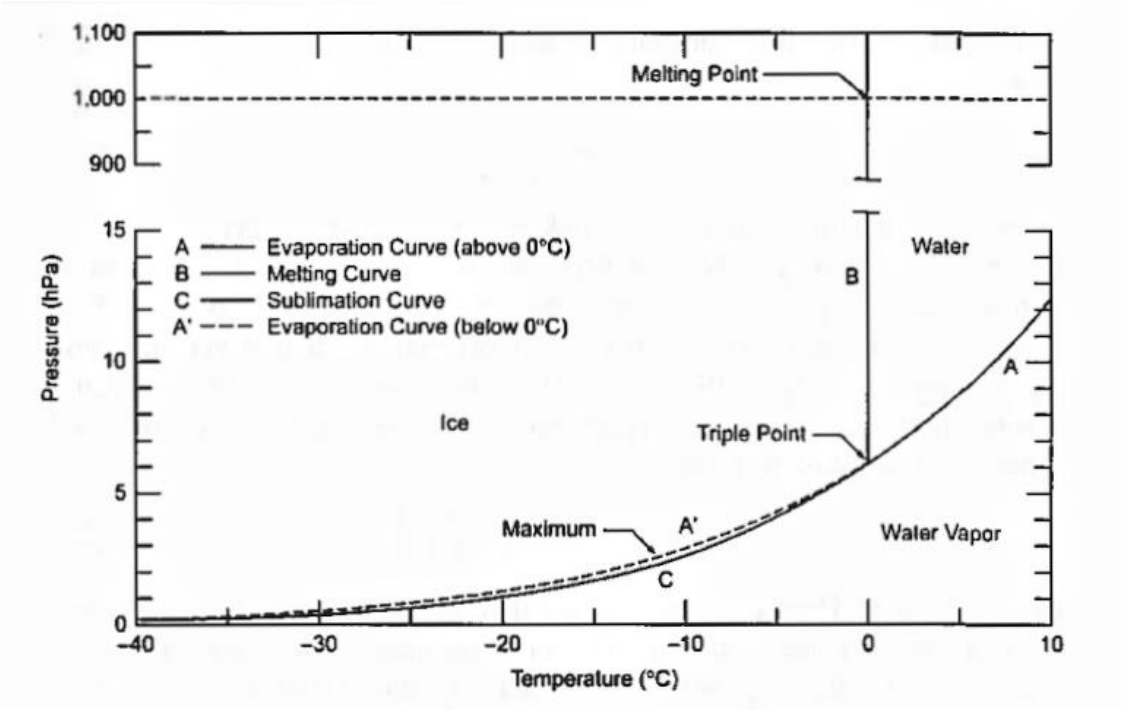

Figure 2: Pressure-temperature phase diagram for water (Armstrong and Brun, 2008)

Heat transfer across the snow-soil interface happens at the bottom of the snowpack. At a depth of about 30 cm the snow is no longer affected by diurnal changes due to radiation (Richard L Armstrong, 1985; Holmgren, 1971). From this depth and down to the snow-soil interface the temperature normally increases with depth, which creates a continuous upwards heat flux (Colbeck, 1983).

Heat transfer by mass change is the energy added to or removed from the snowpack when mass is added or removed (precipitation and snowmelt). This term of the equation is more relevant for energy budget calculations on a glacier than the conditions associated with local surface hoar growth on a snowpack.

The energy balance equation (EQ. 1) applies for energy entering and exiting the snow and does not include the processes of heat transfer in the snowpack. When energy is transferred within the snowpack, two main processes are active: conduction and diffusion of water vapor (Anderson, 1976). Since snow is a porous media, and conduction mainly happens where there is grain to grain contact, the heat transfer by conduction happens at a relatively slow rate. Diffusion of water vapor in the snowpack occurs as sublimation and deposition of vapor in the pore space between the snow grains. Water molecules sublime from snow grain surfaces with relatively too low water vapor pressure and deposits on snow grain surfaces with relatively too high water vapor pressure. The movement of water molecules is largely caused by a water vapor

pressure gradient induced by a temperature gradient. The diffusive process is particularly important in low density snow because the low conductivity of this snow leads to great temperature gradients (Anderson, 1976; McClung & Schaerer, 2006). Due to the difficulty of separating measurements of conduction and diffusion, the heat transfer ability of snow is often referred to as effective thermal conductivity, including both heat transfer mechanisms. In 1992, Sturm & Johnson (1992) published an article where they compared different measured relationships between snow density and effective thermal conductivities (figure 3). The scatter in results between different studies indicates that effective thermal properties may be affected by other factors, such as grain shape and size (Sturm & Johnson, 1992). The effective thermal conductivitie used in this study is within the range of measured conductivities showed in figure 3.

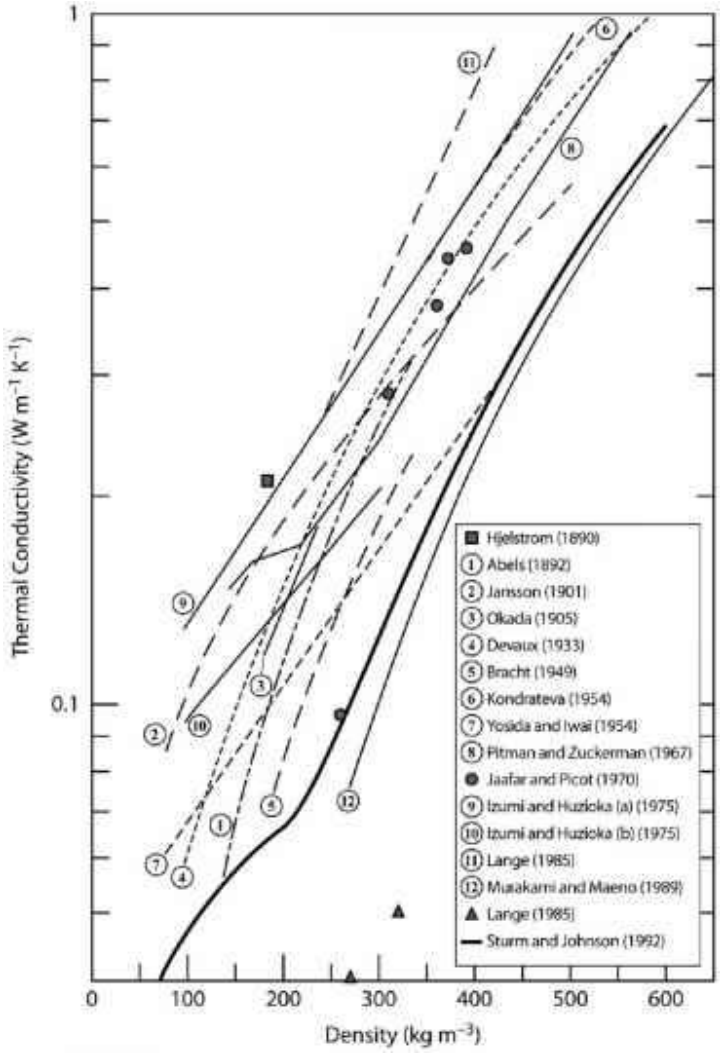

Figure 3: the relationship between effective thermal conductivity and density of snow from several papers. Modified version of a figure from (Sturm & Johnson, 1992).

2.2 Near surface faceted crystals

Faceted crystals are angular shaped snow crystals that are formed in the snowpack (figure 6). Layers of faceted crystals have the potential to be a weak layer that can contribute to avalanche formation. The crystals are anisotropic, meaning they are stronger in one direction. They are resistive to normal stress and weak to shear stress. In addition, they have a low conductivity due to the angular shapes which results in little grain contact. This can result in a lower effective thermal conductivity in this layer compared to other types of snow, and the layer may maintain a higher temperature gradient than the rest of the snowpack. Most significantly, the effect that could destroy facets, rounding of snow grains due to a difference in curvature, is much slower than the effect of metamorphism driven by temperature gradient (faceting). This allows the layer to persist for weeks or months, making it a persistent weak layer.

The morphology of the crystals is a result of undergoing dry snow metamorphism. They become angular due to a high vapor pressure gradient around a snow grain, which is caused by a large temperature gradient around the grain (diffusive process). 25 mb/m is the vapor pressure gradient needed to create faceted crystals in 48 hours (Richard L Armstrong, 1985). A temperature gradient of 200º C/m was observed to produce faceted crystals with sizes up to 1 mm in 36 hours (Birkeland et al., 1998). The temperature gradient necessary to produce a vapor pressure gradient capable of producing faceted crystals (min. 5mb/m) varies with the temperature of the snow (LaChapelle & Armstrong, 1977) (see figure 4). At higher temperatures, the critical temperature gradient is lower. This is the reason faceting is more likely to occur when the temperature is closer to 0°C.

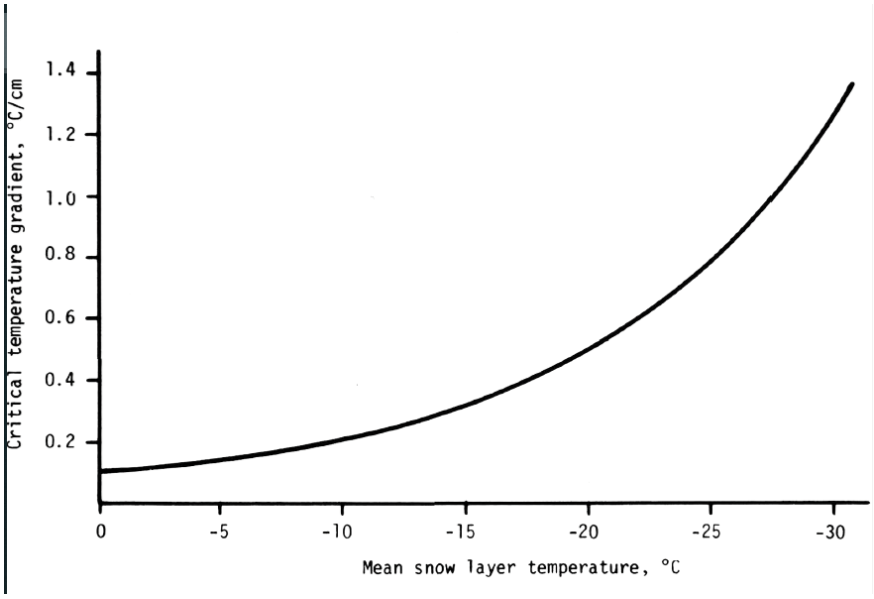

Figure 4: Critical temperature gradient for faceting as a function of mean snow layer temperature (LaChapelle & Armstrong, 1977)

On clear sunny days, solar radiation penetrates through the snow surface and increases the snow temperature just below the surface. This temperature increase can sometimes be large enough to create a melt layer while the surface itself is cooling due to outgoing longwave radiation. This again results in a large temperature gradient in the uppermost few cm in the snowpack. Because of the relatively warm temperature of the melt layer (approximately 0°C) the facets will be produced quickly above this layer, and potentially below if the snow is cold enough. This process of creating faceted crystals is called radiation recrystallization.

A similar process called melt layer recrystallization involves a wet melt layer that is buried by new, colder snow. The wet melt layer (approximately 0°C) is caused by either solar radiation or rain. The cold new snow on top of the warmer melt layer causes a large temperature gradient, which will produce facets at a high rate. The process happens faster if the melt layer has a higher liquid water content or if the new snow layer is thin.

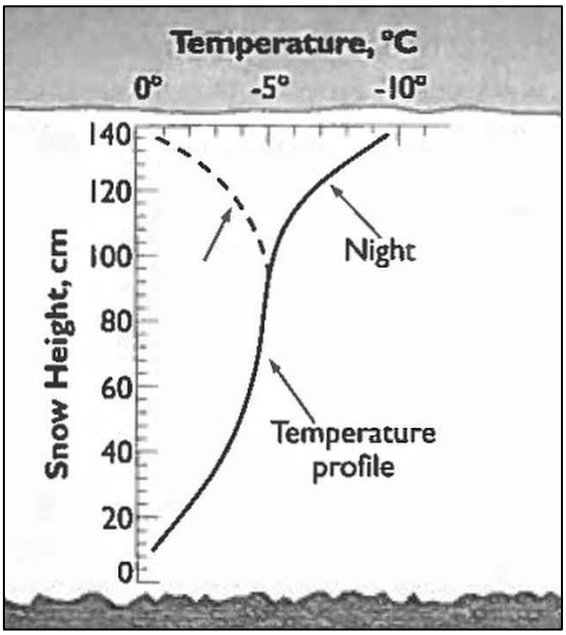

Figure 5: Illustration of diurnal temperature fluctuations in a snowpack (McClung & Schaerer, 2006)

A third faceting process which is more widespread is called diurnal recrystallization. Snow as a material has low conductivity, meaning it works great as an insulator, and temperature changes slowly within the snowpack. As described in the section of the energy balance equation, solar radiation will heat the upper part of a snowpack during the day. In the night, the surface cools as a result of stronger outgoing than incoming longwave radiation. Due to low conductivity, these diurnal surface temperature fluctuations do not reach far down in the snowpack. It has been observed that the temperature 30 cm below the surface remains relatively constant (Richard L Armstrong, 1985). The large temperature fluctuations at the surface creates

a large temperature gradient in the top 30 cm, but the uppermost part of the snowpack will experience the biggest temperature gradient (figure 5). This is where the faceting will occur. In addition, snow at the surface can have very low density due to large pore space, and thus have a lot of area for vapor transport and growth of large faceted crystals. Temperature gradients above 200°C/m have been measured as a result of this effect (Birkeland, 1998).

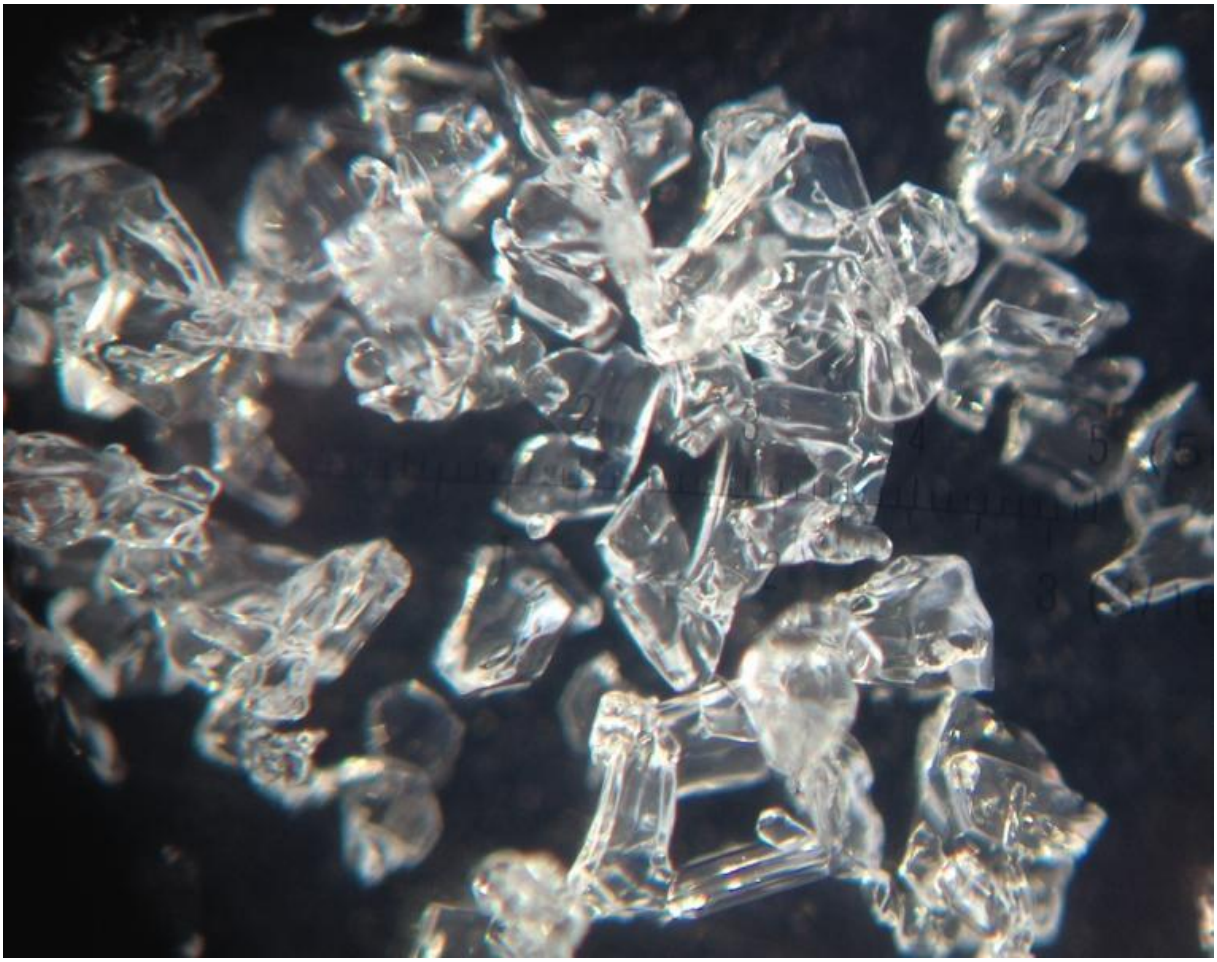

Figure 6: Faceted crystals photographed by Greg Gagne in Salt Lake region in 2013.

All these mechanisms which produce near surface faceted crystals require a cold surface temperature, which is needed in order to create a high enough temperature gradient. The total outgoing heat flux that affects the surface is dependent on different factors. The latent heat release from surface hoar growth could potentially be a source of heat that could reduce the outgoing heat flux, resulting in a lower temperature gradient.

2.3 Surface hoar

Surface hoar are crystals that form on the snow surface. There is a potential avalanche risk related to subsequent burial of a layer of surface hoar. This is because the crystals hold the same anisotropic properties as faceted crystals, as a result of weak bonds between the crystals. When

buried, this anisotropy makes the surface hoar layer a potential sliding surface for slab avalanches. If the layer remains undisturbed and unaffected by e. g. temperature, it remains a potential hazard for a long period, in some cases up to 100 days (Birkeland, 1998; Jamieson & Schweizer, 2000; Stössel, 2007).

Surface hoar is created under cold and clear conditions, when the outgoing longwave radiation dominates the Q_n term of the surface energy balance equation (EQ. 1). This can make the snow surface cooler than the air above. Through several observations on surface hoar growth, Hachikubo and Akitaya (1997) found that the temperature difference between the surface and the air ($\Delta T = T_{air} - T_{surface}$) was at least 5°C when the air temperature was measured at 1m. If locally supersaturated air is present near the surface, the vapor will be deposited on irregularities on the surface because it tries to maintain equilibrium between the atmosphere and the snow, resulting in surface hoar. The latent heat (Q_g) released through deposition of water vapor will result in energy exchange at the snow surface. Due to conductive and diffusive heat transfer, this will also affect the temperature further down in the snowpack.

Surface hoar appears in different shapes, and the morphology is dependent on different factors. Lang et al. (1984) found that needle-like crystals formed at snow surface temperatures below -21°C, while more plate-like shaped crystals were formed when the surface temperature was between -12.5°C and -21°C (figure 7).

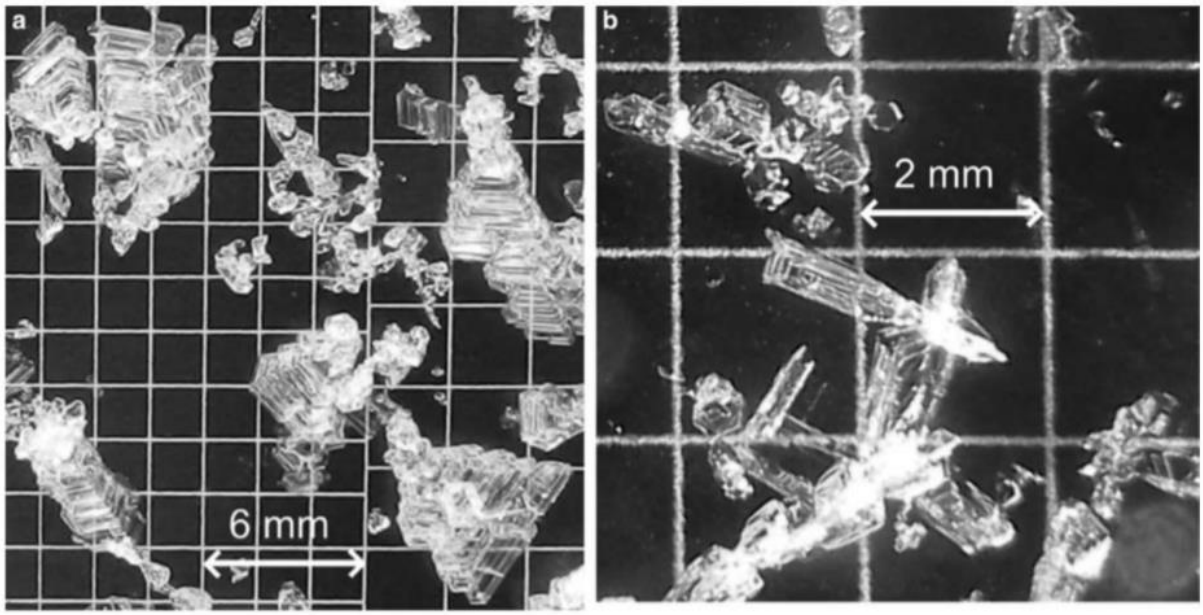

Figure 7: Surface hoar crystals with **a)** plate-like shapes and **b)** needle-like shapes (Horton & Jamieson, 2017).

Since the water vapor from the air is deposited, the air above the surface must remain locally supersaturated in order to keep the surface hoar growing. Lang et al. (1984) assumed that surface hoar was created only through diffusion of water vapor molecules, without the necessity of wind. However, it was later discovered that previously observed surface hoar growth rates could not be formed through diffusion in still air alone (Colbeck, 1988). Some turbulent transfer of water vapor mass is needed to keep the air locally supersaturated with water. According to Hachikubo & Akitaya (1997), surface hoar forms when wind speed is 1 – 2 m/s at 0.1 m above ground. Stössel et al. (2010) measured the wind speed 4 m above the snow surface, and here the wind speed was never higher than 4 m/s when surface hoar were formed. Considering this, the height of the wind speed measurements is an important parameter. As long as the wind speeds stay low, the conditions will be favorable for surface hoar growth. However, if the wind speeds get to high, the wind will have a destructive effect on the surface hoar formation. This is because they affect the sensible heat flux, resulting in a higher temperature at the surface of the snow. A low wind speed will allow for slight vertical turbulence which will supply the air right above the surface with water vapor without increasing the sensible heat to a destructive level (Hachikubo & Akitaya, 1997). As the crystals grow turbulent fluxes increase and given a high relative humidity, surface hoar growth will increase. This shows that surface hoar growth has a positive feedback effect (Hachikubo, 2001).

3. Methods

3.1 Field work and experimental set up

To acquire data of how much surface hoar is created during a night, fieldwork was done at Hollekvebrui in Sogndalsdalen (figure 8). The field locality by Hollekvebrui was chosen due to its flat surface and its proximity (50m) to the river Sogndalselvi, as well as its convenient location close to a road, making it accessible. The river is believed to provide extra humidity to the area and likely enhance the process of surface hoar growth. Additionally, trees located on the northside of the area could shield from strong nocturnal winds down the valley. Altitude of the location is 392 meters above sea level.

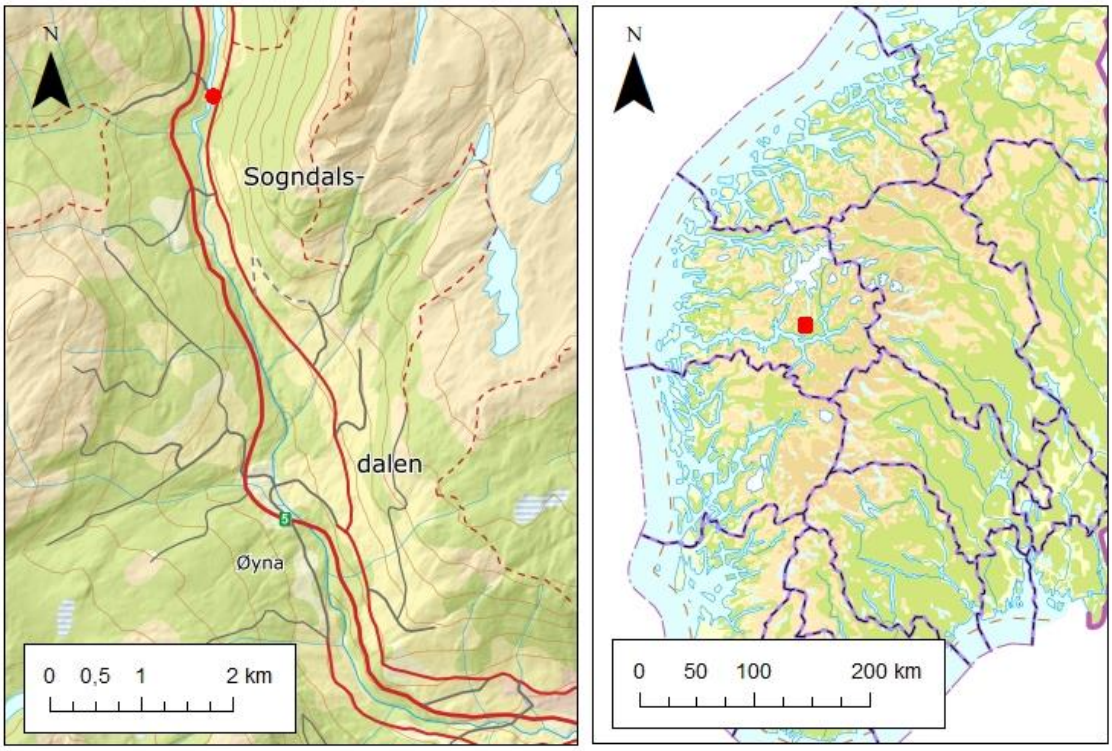

Figure 8: The field locality near Hollekvebrui in Sogndalsdalen, Norway.

Stössel et al. (2010) described a method of measuring surface hoar growth which involved weighing a box containing the uppermost 10 cm of the snowpack in the afternoon (at 16:00) and in the morning (at 08:00). The fieldwork at Hollekvebrui was strongly inspired by this method. A drawer shaped box with three sides and bottom, with volume measurements 0.016 m^3 (40 x 40 x 10 cm), was filled with snow (figure 9). The box was made of 0.6 cm thick Depron, a type of polystyrene with a thermal conductivity of 0.035 W/(m*K), to minimize disturbance of the snow. In the evening, a snow column with surface area 40 x 40 cm was isolated, and the box was pushed into the column to obtain a sample of the 10 uppermost cm of snow. The filled box was weighed and placed in a prepared hole in the snow with same

dimensions as the box, so that the snow sample surface would be level with the surrounding snow surface. Before sunrise the next day the box was weighed again. Assuming no precipitation, the measured accumulated mass equals the mass of surface hoar created between measurements. Since the surface area of the snow in the box is 0.16 m^2, the mass gain was converted to kg/m^2. The weighing was done for all nights from late January to end of March with weather forecasts giving calm and clear conditions and air temperatures below 0°C.

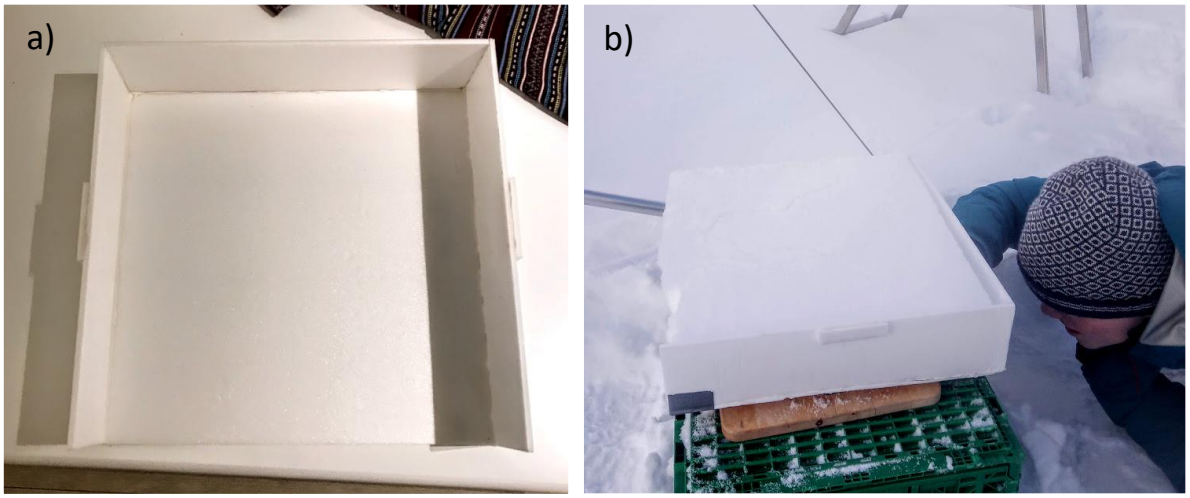

Figure 9: Picture of **a)** the box without snow and **b)** the box with snow in the weighing process.

An automatic weather station (AWS) was placed at the location to measure temperature, wind speed and direction, air pressure, relative humidity as well as incoming and outgoing radiation (see figure 10). Radiation is measured by Kipp & Zonen CNR 4 Net radiometer. Two pyranometer sensors registered incoming and outgoing shortwave radiation, and two pyrgeometer sensors registered incoming and outgoing longwave radiation. The measurements were made at around 2.75 m above ground level, the height being reduced as the snow surface height increased. However, during the observation period the thickness of the snowpack never exceeded 45 cm.

Additional measurements at the site included weather observations and snow pit measurements, with temperature profile, hardness measurements and grain classification. The temperature measurements were done using a digital pocket thermometer (Cooper-Atkins). When digging a snow profile, the first measurements that were done were temperature measurements. This is because the snow temperature will adjust to the air temperature, which could give errors to the measured values. The hardness measurements were done by using a hand hardness test (ICSI hardness classification for snow). Snow grains were classified according to the ICSI snow classification system. The measurements were done both in the evening and in the morning of

nights with clear, calm conditions and temperatures below 0°C. All measurements were done closer than 5 meters to the weather station, and values from the weather station are thus representative for the snowpack where the pit measurements took place.

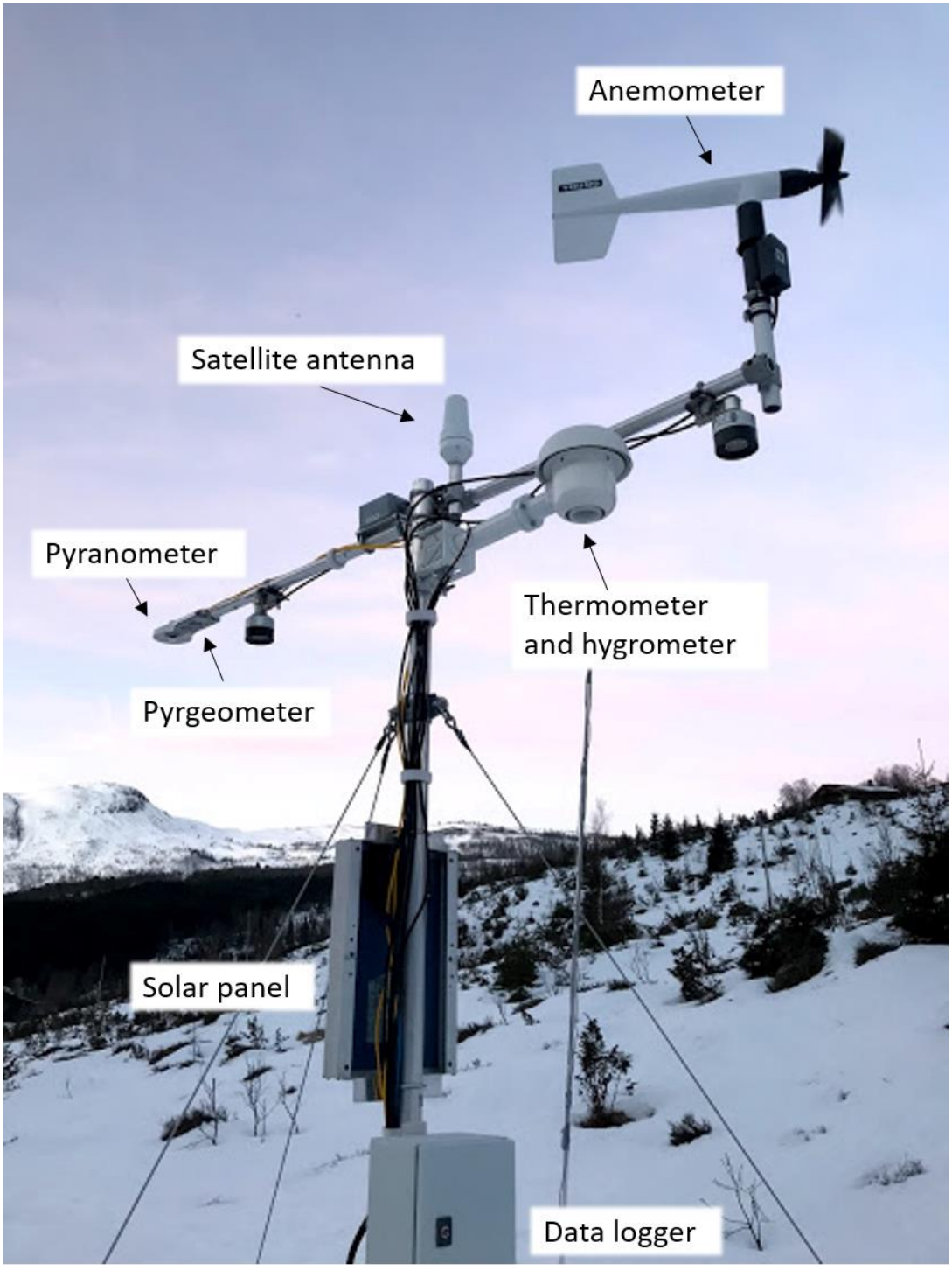

Figure 10: Instrumental setup of the weather station

3.2 Modeling temperature change

3.2.1 Sensible heat release

Due to difficulties related to correct measurements of sensible heat flux, we have chosen to calculate sensible heat using the bulk aerodynamic method. Other calculation methods may also be used, but the bulk transfer method only needs one wind measurement height, which is the case for our measurements at Hollekvebrui. The bulk transfer method assumes horizontally homogenous conditions and constant fluxes with height, which might not be the case, especially since our field measurements are taken in a valley. The calculations are often inaccurate due to the difficulty in choosing the right coefficients (Hock, 2005).

Sensible heat flux q_h can be calculated using the bulk transfer method (Hachikubo, 2001):

$$q_h = C_h c_a \rho_a u_z (T_z - T_s) \tag{3}$$

Where C_h is the bulk transfer coefficient of heat, c_a is the specific heat capacity of air, ρ_a is the density of air, u_z is the wind speed at height z, T_z is the temperature at height z and T_s is the temperature at the surface. The bulk transfer coefficient for the sensible heat C_h is found by adjusting the bulk transfer coefficient in neutral conditions C_N:

$$C_h = C_N(1 - 5R_B)^2 \quad \text{when } 0 \leq R_B \leq 0.2 \tag{4}$$

A value of $3.3*10^{-3}$ was used for C_N, which is the same value used in Hachikubo (2001). The Bulk Richardson Number R_B is:

$$R_B = \frac{g * (T_z - T_s) * z}{T_m * {u_z}^2} \tag{5}$$

z is the elevation in which the measurements are made and is given in meters. The gravitational constant is g, and T_m is the mean temperature in the air in Kelvin (T_z + 273.15). The Bulk Richardson Number R_B is a dimensionless number used to categorize atmospheric stability in the lowest layers of the atmosphere. The numerator in equation 5 represents buoyant forces, and the denominator represents mechanical forces. Unstable conditions with a strong lapse rate will give a negative R_B value, and stable conditions with an inversion will give positive values (see figure 11) (Oke, 1995).

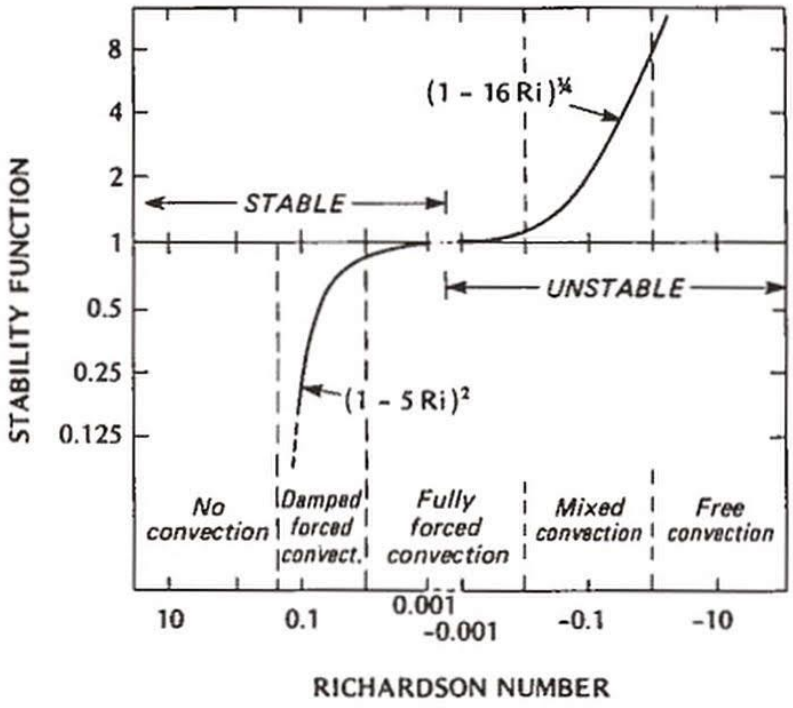

Figure 11: Stability, as a function of Richardson Number (Oke, 1995).

3.2.2 Latent heat release

For a given mass of surface hoar (m_{sh}), the released latent heat (Q_L) is given by:

$$Q_L = m_{sh} L_S \tag{6}$$

Where L_S is the latent heat of sublimation of ice at 0°C. If it is assumed that the temperature of the surface is colder than the water vapor, an additional amount of heat ($Q_{\Delta u}$) is released. This heat is given by:

$$Q_{\Delta u} = C_P \, m_{sh} \Delta u \tag{7}$$

Where C_P is the specific heat capacity of snow and Δu is the temperature change of the surface hoar crystals. If the two values of Q is added together, the total amount of heat that is released through formation of surface hoar (Q_{SH}) can be found. It is assumed that all of this is applied to the snowpack. This is given by:

$$Q_{SH} = Q_L + Q_{\Delta u} \tag{8}$$

To find what temperature change this amount of heat will result in, equation 9 is used.

$$\Delta u_{SP} = \frac{Q_{SH}}{m_{SP} * C_P} \tag{9}$$

Δu_{SP} is the average temperature change in the snowpack, Q_{SH} is the heat provided from the deposition of surface hoar and m_{SP} is the mass of the snowpack. The mass of the snowpack, m_{SP}, is given by the term:

$$m_{sp} = V * \rho_s \quad (10)$$

Where V is the volume of the column and ρ_s is the density of snow.

For a simple calculation we assumed that the temperature 30 cm own in the snowpack remains constant due to no diurnal fluctuation (Richard L Armstrong, 1985). The top of the snowpack will undergo the largest temperature change. To simplify this heat distribution, we assumed that the heat change is zero at 30 cm depth, equal to equation 9 at 15 cm and twice that value at the surface. The doubling value on the surface is a result of choosing a linear temperature gradient where there is zero change at 30 cm depth.

3.2.3 Finite difference method

Temperatures measured by Birkeland et al. (1998) show that the temperature gradients are not linear in the upper 20 cm of the snowpack but is rather curved as illustrated in figure 5. This is because of the low conductivity of snow that poorly transports the heat up and down in the snowpack, resulting in a surface that is cooling and warming more rapidly than the underlying snow. To investigate the curved temperature gradient developing through the night, a numerical model where the snow properties are applied would allow us to simulate the slower cooling further down in the snowpack. The heat equation in one dimension can be used to compute the heat exchange through a volume of snow (Anderson, 1976). The heat equation is a version of the diffusion equation where the thermal diffusivity is assumed to be constant with respect to temperature. The heat equation can be written as:

$$\frac{\partial u}{\partial t} = \alpha \frac{\partial^2 u}{\partial x^2} \quad (11)$$

Where: u = temperature (K)

t = time (s)

x = depth of snow (m)

α = thermal diffusivity (m^2/s)

Thermal diffusivity (α) may be derived from thermal conductivity (k), density (ρ_s) and specific heat capacity of snow (C_P):

$$\alpha = \frac{k}{\rho_s C_P} \quad (12)$$

As mentioned in the section of heat transfer in the snowpack, heat is not only conducted through grain to grain contact but is also transferred through vapor diffusion. In order to include this

effect, Anderson (1976) suggests adding an additional diffusion term on the right side of equation 11:

$$\frac{\partial u}{\partial t} = \alpha \frac{\partial^2 u}{\partial x^2} + \frac{L_S\, m}{\rho_s\, C_p} \tag{13}$$

Where L_S is latent heat of sublimation and *m* is the net amount of vapor that undergoes phase change. When computing heat exchange in the snowpack, we used an effective thermal conductivity (k_{eff}). Values used are based on measured values published by Sturm & Johnson (1992). This way, the additional term of diffusion in equation 13 is not needed.

In order to solve the heat conduction equation, we have used the finite difference method. This is a method where the snow column is split up into a finite number of segments (Δx), and the evolution of the temperature distribution is calculated for a time interval (Δt). Some approximations have been done in order to solve this numerically:

For a forward difference in time, the derivative on the left side of the equation (EQ. 13) is replaced by a term with the difference in temperature (u) at a point (x) over a given time interval (Δt). This approximation includes an error of order Δt, which becomes negligible when the time interval is small enough. The forward difference in time is given by:

$$\frac{\partial u}{\partial t} \approx \frac{u(x, t + \Delta t) - u(x, t)}{\Delta t} \tag{14}$$

For a central difference in space, the second order derivative on the right side of the equation (EQ. 13) is replaced by a term with the difference in temperature (u) over a given space interval (Δx) squared. This term is derived from using Taylor series expansion around a point x, using the solution for points (x-Δx) and (x+Δx). This approximation includes an error of order Δx^2, which becomes negligible when the space interval is small enough. The central difference in space is given by:

$$\frac{\partial^2 u}{\partial x^2} \approx \frac{u(x + \Delta x, t) - 2u(x, t) + u(x - \Delta x, t)}{\Delta x^2} \tag{15}$$

By substituting equation 14 and 15 into the heat equation (EQ. 11), and solving for the temperature at a point (x) at the next timestep (t+Δt), we get:

$$u(x, t + \Delta t) = \alpha \frac{\Delta t}{\Delta x^2}\big(u(x + \Delta x, t) - 2u(x, t) + u(x - \Delta x, t)\big) + u(x, t) \quad (16)$$

When solving the heat equation numerically in an Excel spread sheet, equation 16 is essentially what is used for every cell in the model, with some exceptions (boundary conditions). Due to the formula being dependent on three points along the x-axis at a previous time, it will not have all input needed at t = 0, x = 0 and x = max. In these cells some predetermined conditions are needed:

For the case of t = 0, an *initial condition* (IC) has been implemented. This is the initial temperature in the model. In our first computations using the heat equation, we assumed an IC where the initial temperature gradient was linear between the top (x_0, t_0) at -10°C and the bottom (x_{max}, t_0) at -4°C.

The bottom of the modelled snow column (x = max) was set to 0.3 meters, which is the depth where we assume temperature to not be affected by diurnal fluctuations (Richard L Armstrong, 1985). Since a constant temperature was assumed, these cells were given a *Dirichlet boundary condition* (fixed boundary condition), with a constant input value for each time step:

$$u(x_{max}, t) = T_{iso} \quad (17)$$

$T_{íso}$ is a given constant temperature at the isothermal boundary. This boundary condition (BC) allows energy to move freely in and out of the system. Colder temperatures above the isothermal boundary will give a heat flux into the system, representing the Q_g term of the surface balance equation (EQ. 1).

For the upper boundary at the snow surface, a *Neumann boundary condition* was used. This boundary condition is often referred to as a heat flux boundary condition and is used when the heat flux is known. For a finite difference model, an approximation of the boundary condition at x=0 is needed:

$$\left.\frac{\partial u}{\partial x}\right|_0 = \nabla u \approx \left.\frac{\Delta u}{\Delta x}\right|_0 = \nabla u \quad (18)$$

Where ∇u is temperature gradient in K/m in the vertical direction, calculated from Fourier's law of heat conduction with heat flux q and effective thermal conductivity k_{eff}:

$$q = -k_{eff}\nabla u \tag{19}$$

We have solved the upper boundary condition using a three-point method using the points (x_0), ($x_0+\Delta x$) and ($x_0-\Delta x$). The average temperature gradient between these points will be the temperature gradient that we calculate based on data collected. The approximation with these three points is:

$$\frac{[u(x_0 - \Delta x, t) - u(x_0, t)] + [u(x_0, t) - u(x_0 + \Delta x, t)]}{2\Delta x} = \nabla u \tag{20}$$

The points (x_0) and ($x_0+\Delta x$) both have equation 16, and thus are not controlled. The point ($x_0-\Delta x$) is a fictitious cell added in order to manipulate the temperature gradient ∇u. Solving for u($x_0-\Delta x$, t) gives:

$$u(x_0 - \Delta x, t) = 2\Delta x\, \nabla u + \mathrm{u}(x_0 + \Delta x, t) \tag{21}$$

This equation will give us the fictional value needed in order to get the correct average temperature gradient. In this way, when the surface temperature u(x_0, t+Δt) is calculated for the next time step (t+Δt), taking data from u($x_0-\Delta x$, t), u(x, t) and u($x_0+\Delta x$, t), the correct amount of heat is lost from (t) to (t+Δt). In equation 21 ∇u is given in °C/m.

Some problems do arise with using the finite difference method. Due to the approximations made, roundoff errors can lead to overestimation or underestimation of the answer in a single cell. If these errors are too large, they can amplify and ruin the computation. In order to avoid amplification, the depth segments must be large enough and the time steps must be small enough. In a Von Neumann Stability Analysis the relationship between these values can predict if a model will run with or without amplification. The requirement for a stable model is given by:

$$r = \alpha\frac{\Delta t}{\Delta x^2} \leq \frac{1}{2} \tag{22}$$

3.2.4 Calculating vapor pressure

We used the same method to calculate vapor pressure as Birkeland et al. (1998). As Birkeland explains, this method assumes that the pore spaces between the snow grains are saturated with water vapor with respect to ice at the current temperature. Vapor pressure was calculated using the Goff-Gratch formulation (Birkeland et al., 1998):

$$\log_{10} e_i = -9.09718\left(\left(\frac{T_0}{T}\right) - 1\right) - 3.56654 \log_{10}\left(\frac{T_0}{T}\right) + 0.876793\left(1 - \left(\frac{T}{T_0}\right)\right) + \log_{10} e_{io} \quad (23)$$

Where: e_i = saturation vapor pressure of a plane surface of pure ice

T = absolute temperature (K)

T_0 = ice-point temperature (273.16 K)

e_{io} = saturation pressure over pure ice-point temperature (6.1071 mb)

4. Results and discussion

4.1 Field results from 18th to 19th of March

Throughout our whole observation period (late January to end of March) the only night with both visible and measurable surface hoar was the night of 18th to 19th of March. The residual field days are described in appendix III. Weighing of the box and temperature measurements of the snow were conducted at 17:30 the 18th and at 06:20 the 19th. There was a mass gain of 15 ± 1 g on the box, which converts to 94 ± 6 g/m^2. The margin of error is due to the sensitivity of the scale. Temperature profiles from 18th and 19th with snow stratigraphy are included in figure 12.

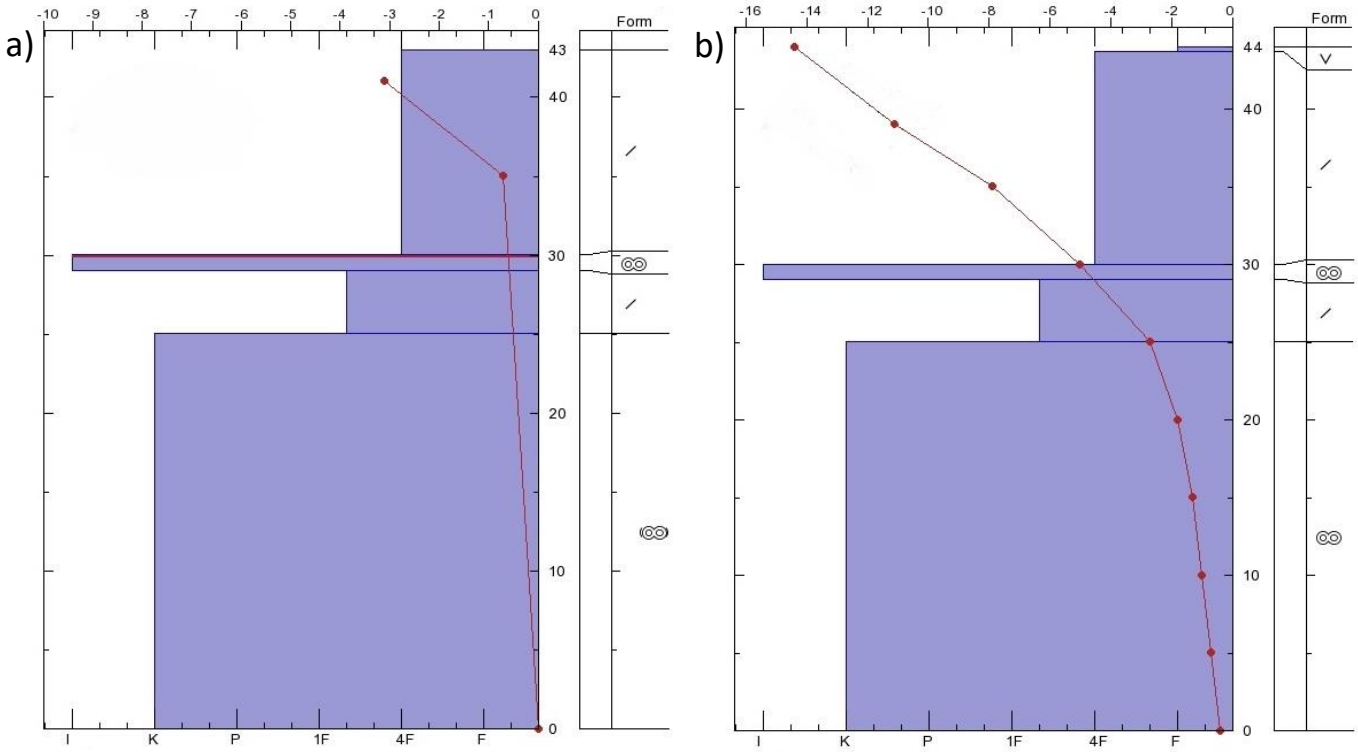

Figure 12: Temperature profile and stratigraphy of the snowpack at **a)** 17:30 the 18th of March and **b)** 06:20 the 19th of March.

Weather data from the weather station shows a relative humidity of about 80-90%. Air temperature varied from 0°C at 17:30 to -11°C at 06:20. Net longwave radiation varied between -33 and -63 W/m^2. Wind speed varied between 0.12 m/s and 1.9 m/s. The variations of net longwave and wind speed during the night can be seen in the figures 13 and 14. Relative humidity, longwave radiation and wind speed are single measurements registered every 10 minutes.

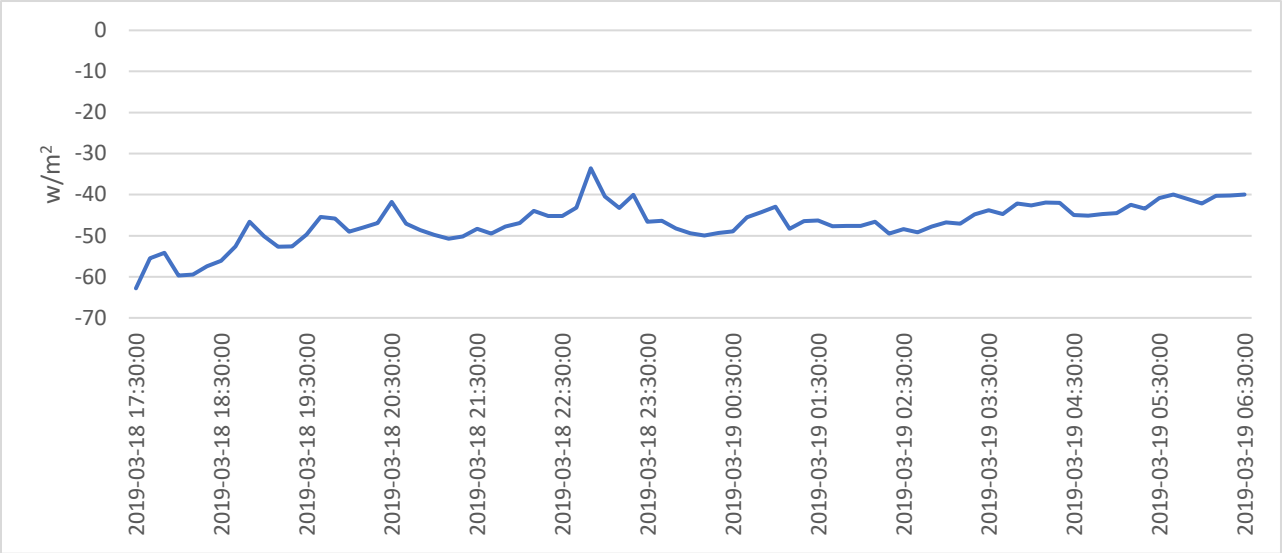

Figure 13: Measured net longwave radiation from 17:30 the 18th of March to 06:30 the 19th of March.

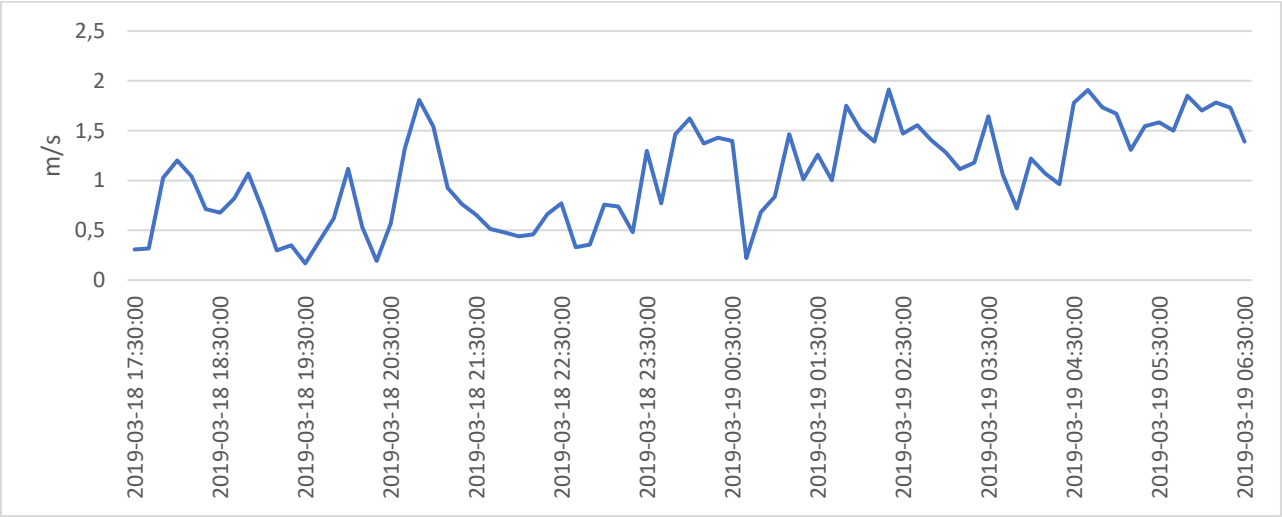

Figure 14: Measured wind speed from 17:30 the 18th of March to 06:30 the 19th of March.

4.2 Development of the temperature model

As earlier mentioned, latent heat release through formation of surface hoar could influence the temperature gradient in the snowpack. In the process of building the model, we started with a simplified version where we only focused on how much cooler the snowpack would have been without surface hoar growth. The development of the temperature model is divided into four steps. The first three steps show how much colder the snow would have been without surface hoar growth (latent heat), by releasing the total Q_{SH} through the upper boundary. The model in step four used weather data to include the other parts of the surface energy balance equation (EQ. 1), as well as mass gain of surface hoar for the latent heat. This resulted in a model where the effect of surface hoar formation can be evaluated with respect to the other terms.

Properties used for the snow in the model are shown in table 1. These are fixed values chosen for the purpose of making the models comparable and having simplified terms to make sure calculations work as expected. The density of snow varies with crystal form and water content, but we have chosen a constant value to 200 kg/m^3, which is within the boundary values for new and decomposing snow (R.L. Armstrong & Brun, 2008). The range of measured effective thermal conductivity is shown in figure 3, and with a density of 200 kg/m^3 we have used an effective thermal conductivity of 0.1 W/(m*K). A specific heat capacity of 2090 J/(kg*K) was chosen as constant, which is the specific heat capacity of ice at -5°C. The initial condition (IC) was set to be linear between -4°C at the isothermal boundary at 0.3 m and -10 °C at the surface. The temperatures through a snowpack at sunset (used as IC) can vary between locations and through the season, so we chose the temperatures from a measurement made by Jordan, O'Brien, & Albert (1989). The mass of surface hoar that we used for the model (0.18 kg/m^2) was the maximum mass measured by Stössel et al. (2010).

Table 1: Values chosen for developing the model

Description	Values	Variation	Source
Density of snow, ρ_s (kg/m^3)	200	20 - 700	Armstrong and Brun, 2008
Effective thermal conductivity, k_{eff} (W/(m*K))	0,1	0,04 - 0,98	Sturm and Johnsson, 1992
Specific heat capacity snow, C_P (J/kg K) at temperatures from 0°C to -20°C	2090	1959-2108	Gray and Male, 1981
Isothermal boundary depth (m)	0,3	0,2 - 0,3	Armstrong, 1985, Birkeland, 1998
Temperature at isothermal boundary (lower BC) (°C)	-4	-	Example value from Jordan et al., 1989
Initial surface temperature of snow (°C)	-10	-	Example value from Jordan et al., 1989
Total time (12 hours), t_{tot} (s)	43200	-	-
Surface hoar created (kg)	0,18	0 – 0,18	Stössel et.al, 2010
Depth intervals, Δx	0,02	-	-
Time intervals, Δt	300	-	-

4.2.1 Constant heat release from surface

Initially, the model was run using the simple assumption of a constant heat release throughout the night implemented with the Neumann boundary condition (EQ. 21) at the surface of the snowpack. This is illustrated by the horizontal line (orange) in figure 19. The temperature gradient ∇u in equation 21 was calculated with equation 19, where the heat flux q is:

$$q = \frac{Q_{SH}}{t_{tot}} \tag{24}$$

Where Q_{SH} is total energy released per square meter due to surface hoar growth, and t_{tot} is time between measurements in seconds. With 0.18 kg of surface hoar and 12 hours total, the upper

boundary condition uses an outgoing heat flux of 11.89 W/m^2 (shown in figure 19). Constants used are showed in table 1. The modelled hourly temperature change during the night is showed in figure 15. The graph shows that the temperature steadily decreases with time, ultimately reaching a surface temperature of -21.3°C.

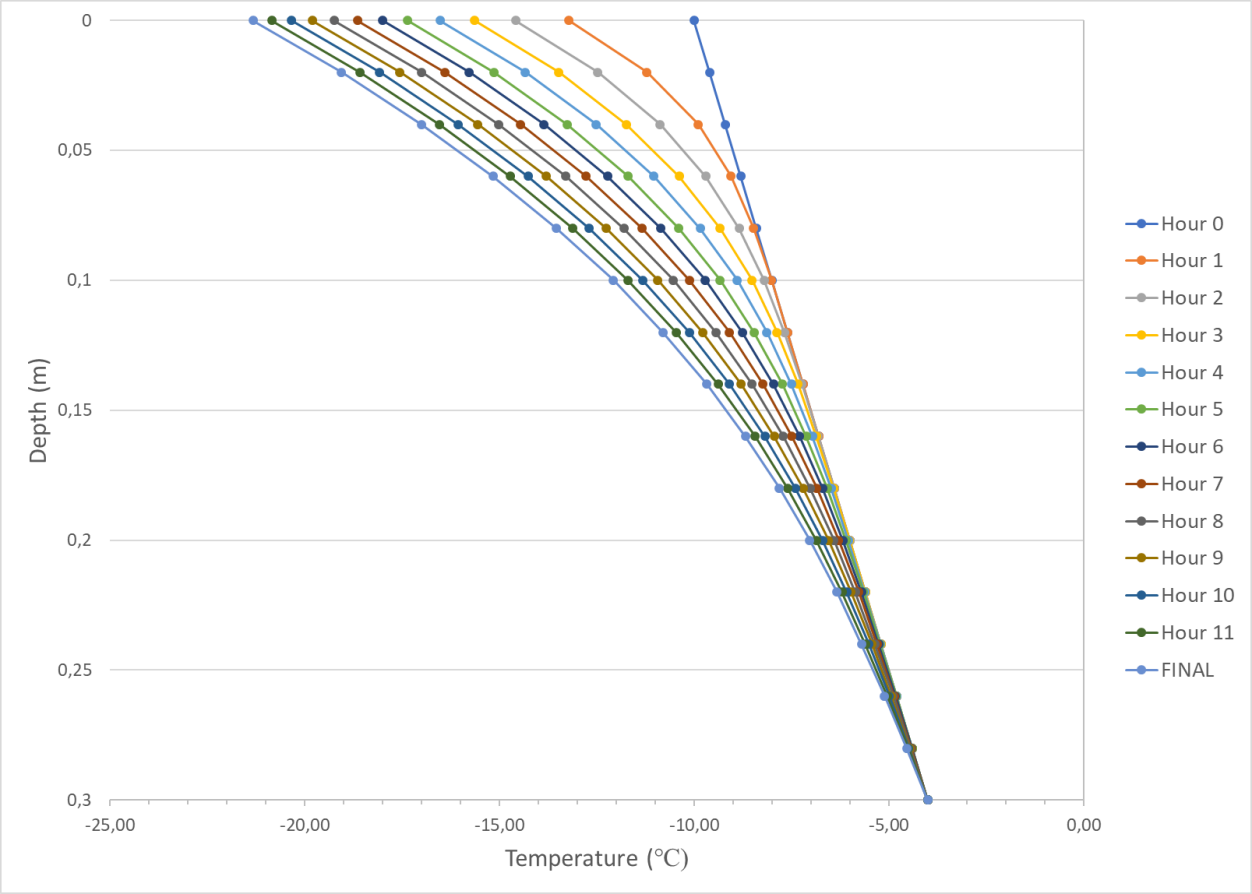

Figure 15: Hourly temperature change in the initial modelled snowpack. Heat flux is constant. The final temperature calculation is at 12 hours.

With a constant heat release, the highest temperature gradient (= 122.58°C/m) is at 0 – 1cm depth and at the end of our calculations (after 12 hours), as seen in figure 20. If the surface hoar affects the temperature gradient mostly in the end of the night, instead of the beginning of the night, this is of less importance because temperatures are lower towards the end of the night. This would produce lower vapor pressure gradients, and the conditions would be less suitable for faceting. However, since the temperature gradient changes the most in the first two hours, and changes more gradually for the remaining 12 hours, this will result in the highest vapor pressure gradients somewhere in the beginning of the night.

4.2.2 Linearly changing heat release

A constant heat flux may not be realistic because outgoing longwave radiation will vary during the night. Given clear stable conditions, the outgoing longwave radiation will increase quickly

after the sun has set, which leads to a rapid cooling of the snow surface. This could give most of the surface hoar growth in the beginning of the night. Because the total heat from surface hoar growth is known, a linear model is the next simplest step to solve for this difference in outgoing heat flux. Assuming the heat flux is not constant, but rather a linear function with a high heat release in the beginning of the night and lower towards the end, equation 21 can be modified to:

$$u(x_0 - \Delta x, t) = 2\, f(t) + \; u(x_0 + \Delta x, t) \tag{25}$$

Where f(t) is the linear function

$$f(t) = (\Delta x\, \nabla u)\, y - \left((\Delta x\, \nabla u) \frac{t}{t_{tot}} * 2(y - 1) \right) \tag{26}$$

t is the timestep and t_{tot} is the total time in seconds. ∇u is calculated as in the initial model. y is a value between 1 and 2 that shows how much higher the heat release is in the beginning of the night. If y=2, the heat release at t_0 is twice the average heat release calculated in equation 24. As t approaches t_{tot} the heat release decreases, and at t_{tot} the heat release is 0 (with y=2). If y is 1.5, the heat release at t_0 is 1.5 times average heat release, and the heat release at t_{tot} is 0.5 times average heat release. The model shows that higher values for y can be problematic as the heat release becomes too large and the surface starts warming up before the night is over, but this is dependent on Q_{SH}. High Q_{SH}-values will allow for a higher y, without warming the surface. See figure 16 for the temperature change when modelling with 180 grams of surface hoar and a y-value of 2. For the case of 180 grams of surface hoar formation with a 12-hour period, y-values over 1.3 will produce situations where temperatures in the snow increases. We chose a y-value of 1.2225 when modelling the second time. The hourly temperature change using y = 1.2225 is showed in figure 17.

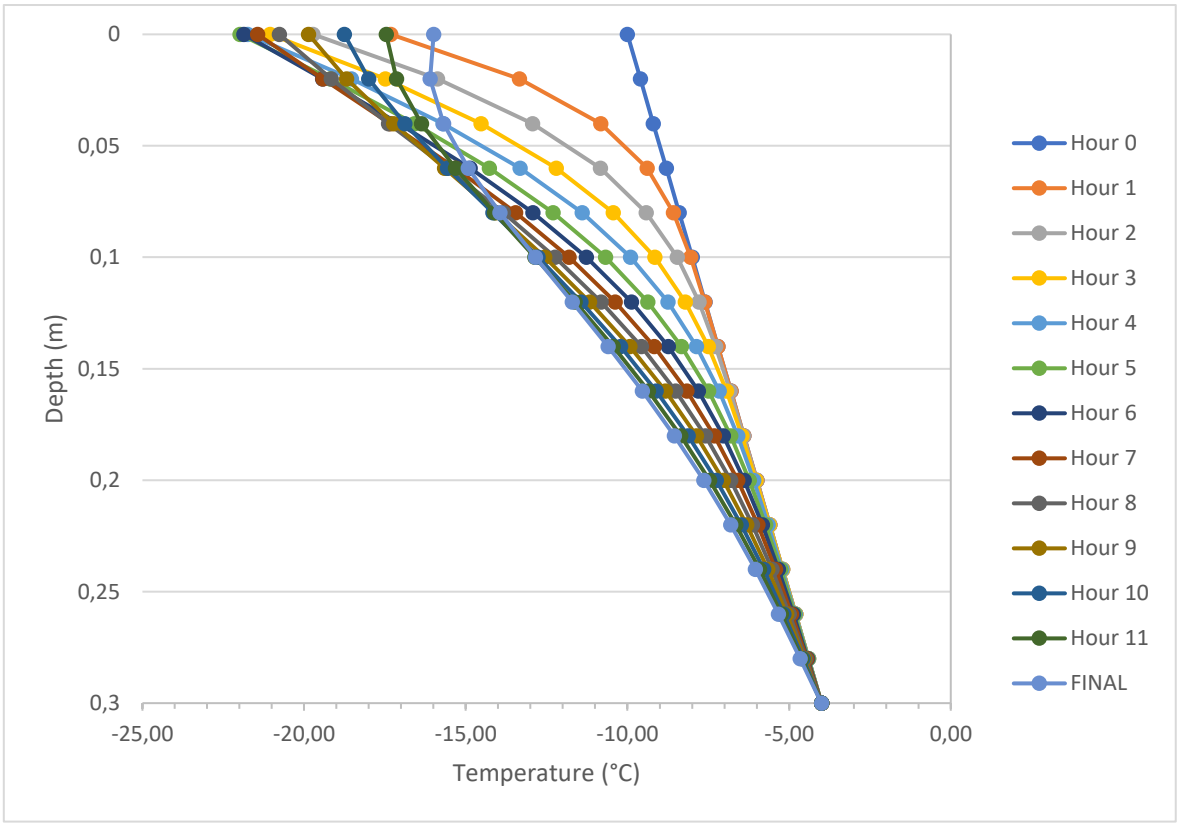

Figure 16: Illustration of linear heat release where y = 2. The surface becomes warmer after the halfway mark. The final temperature calculation is at 12 hours.

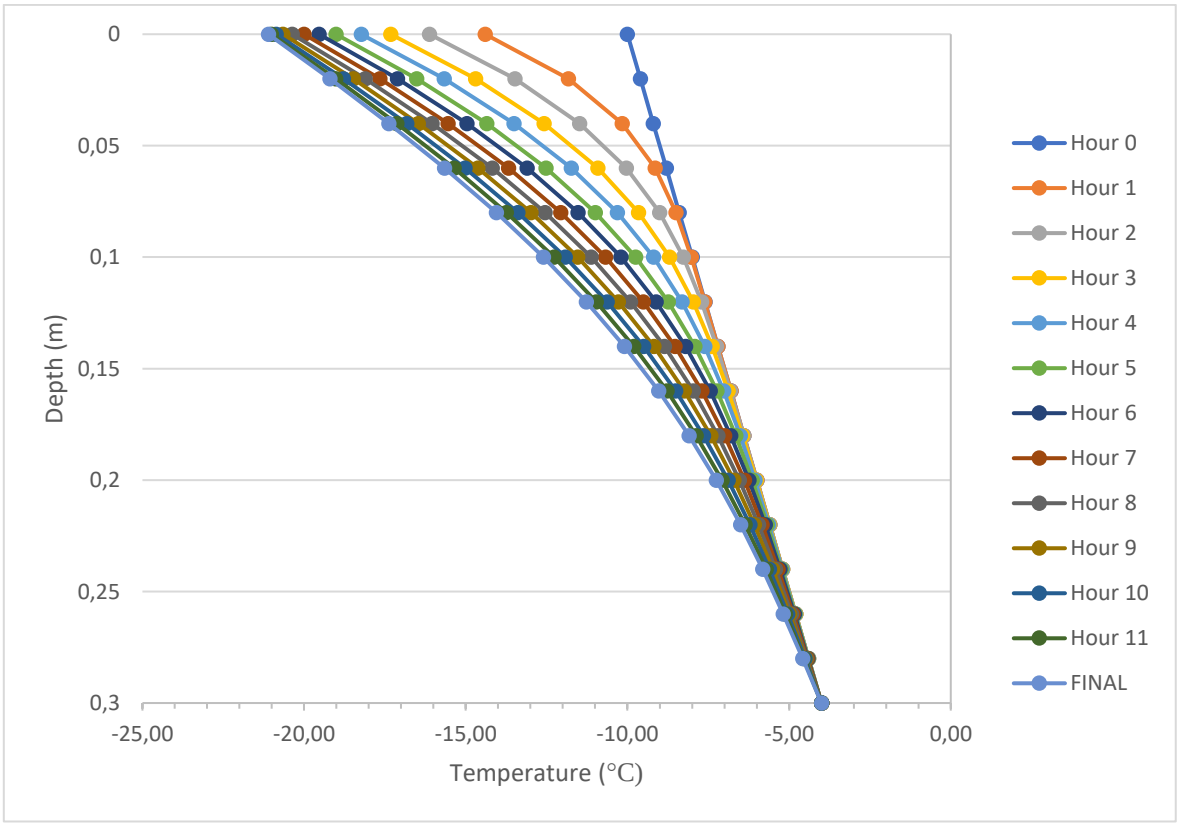

Figure 17: Hourly temperature change in the initial modelled snowpack. Heat flux is linear and the y-value from equation 26 is 1.2225. The final temperature calculation is at 12 hours.

With a linear heat release the highest temperature gradient is at 0 – 1 cm depth after 2 hours, as seen in figure 20. The highest temperature gradient is 132.1 °C/m. This result is interesting because at the beginning of the night the temperature gradient becomes steep due to rapid cooling after sunset. A high temperature gradient including relatively high temperatures give favorable conditions for faceting due to high vapor pressure gradients. If surface hoar grows mostly in the beginning of the night, as this heat flux suggests, the favorable conditions might be destroyed. The linear model does also have the strongest temperature gradient of the three listed. Because the outgoing heat is linear it could be thought that the facets could disappear when the temperature gradient becomes smaller than average when the half the time has passed. This is however not the case, due to the processes related to persistence of faceted crystals.

4.2.3 Heat release dependent on surface temperature

The linear heat release in the last model is possibly not realistic. The surface hoar growth might follow the same pattern as outgoing longwave radiation. Stefan-Boltzmann's law (EQ. 2) states that any object with a temperature above 0 K will emit longwave radiation, and this radiation is correlated with temperature of the surface of the object. We have modified equation 21 to include Stefan-Boltzmann's law, so that the heat release at the upper boundary condition due to no surface hoar growth is dependent on temperature at the surface x_0 in the fourth power. This way, the heat release is largest in the evening, before the surface cools. Due to snow having an emissivity of 0.985-0.99 (Dozier & Warren, 1982) we have assumed the emissivity to be 1 for simplification. The equation for the imaginary cell is changed to:

$$u(x_0 - \Delta x, t) = 2\, f(u) + \; u(x_0 + \Delta x, t) \tag{27}$$

where:

$$f(u) = -\frac{\sigma\,(u(x_0, t) + 273.15)^4\,\Delta x}{k_{eff} * R} \tag{28}$$

The total energy released is still the same as the energy from surface hoar growth. R is a ratio number used to adjust the Stefan-Boltzmann radiation flux to fit the amount of total energy from surface hoar (Q_{SH}). This ratio number was obtained by running the model with equation 27 and dividing the total radiation flux energy by the surface hoar energy (Q_{SH}). When running the model with the ratio number obtained (R ~ 20.518) the surface temperature dropped, and the modelled energy changed to a number close to the energy form surface hoar formation. Because the upper boundary condition includes two cells (x_0 and $x_0+\Delta x$) that use the heat

equation, a lowering of the heat flux will give a slower temperature change from one t to the next. This gives a lower total modelled energy than desired. The solution to this error is to run the model several times, and each time adjusting the R-value. After three rounds of calculating a ratio number, we got a difference of < 0.01% between modelled radiation energy and surface hoar energy with the ratio number of R ~ 20.499. The modelled hourly temperature change using equation 27 with this ratio number is showed in figure 18. The heat flux at the surface is shown in figure 19.

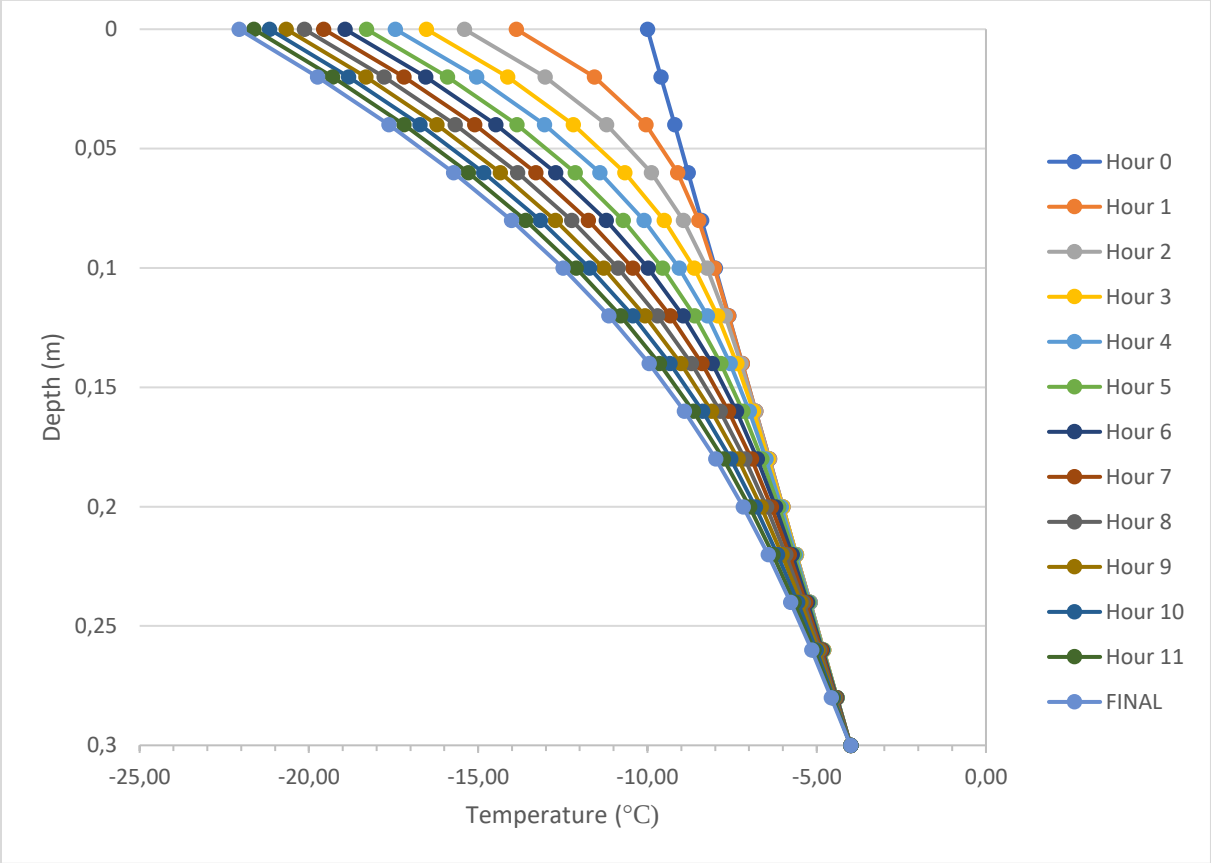

Figure 18: Hourly temperature change in the initial modelled snowpack. Heat flux is varying with time.

With a heat release changing with surface temperature the highest temperature gradient is at 0 – 1 cm depth after 3 hours and 40 minutes, as seen in figure 20. The highest temperature gradient is 110.68°C/m, which is lower than both the constant and the linear model. If the surface hoar growth is dependent on the surface temperature, it will have less effect on temperature gradients in the snowpack compared to the linear and constant model.

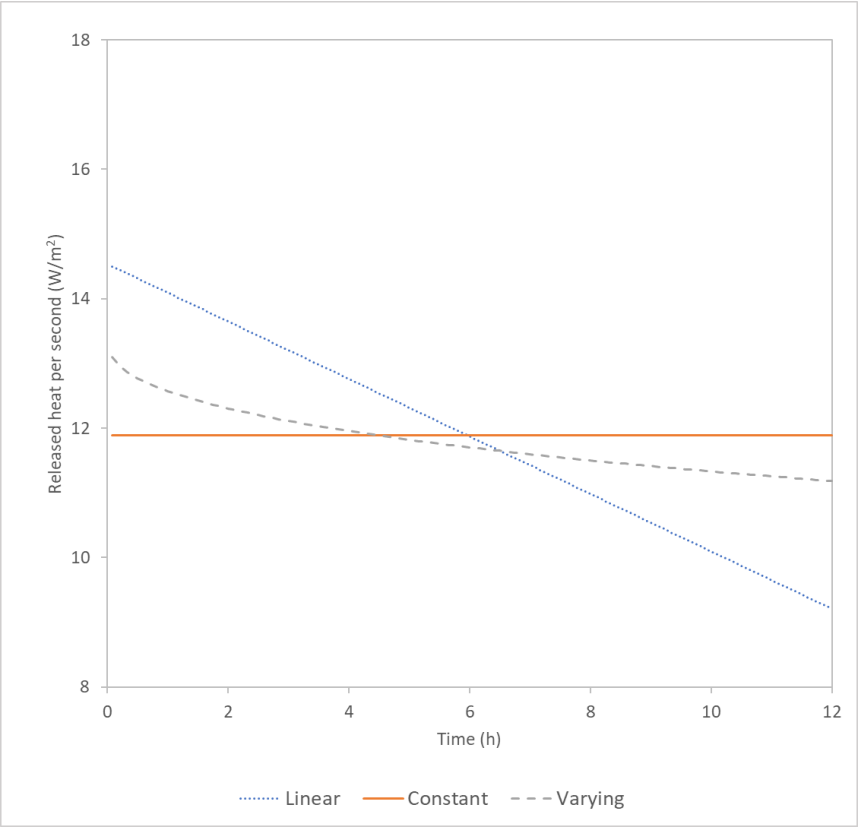

Figure 19: Graphs showing how the heat is released in the different models. The total heat released is the same (513 720 J for 0.18 kg of surface hoar) in all models, but the heat flux distribution differs.

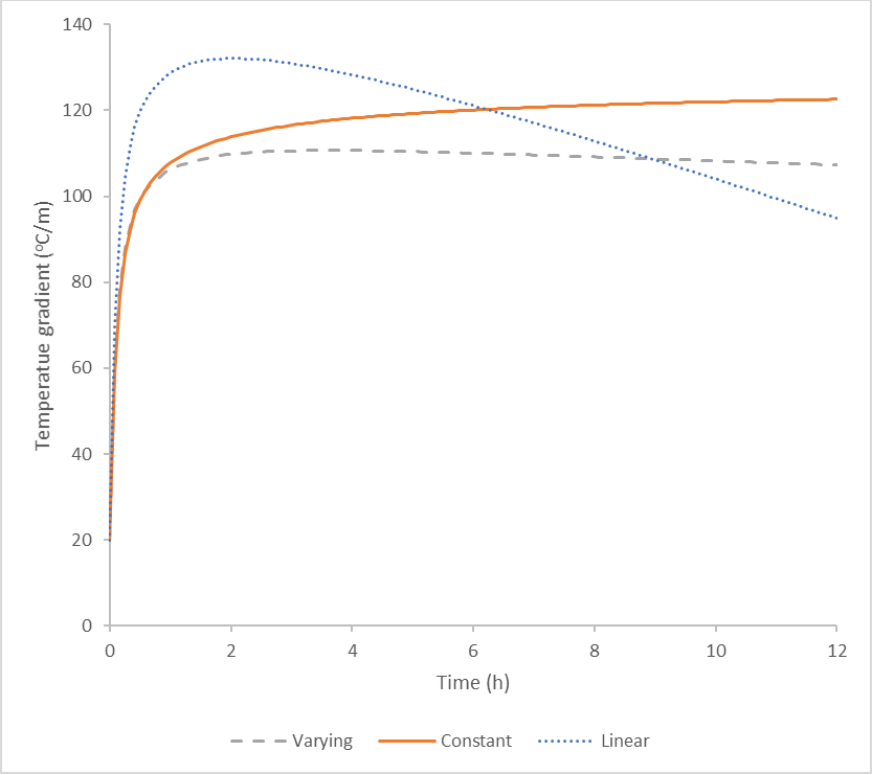

Figure 20: Graphs showing the variation in temperature gradient in the snow right below the surface. The constant model reaches its highest temperature gradient at the end of the simulation (12 h). The linear model reaches its highest temperature gradient after 2 hours. The varying model reaches its highest temperature gradient after 3 hours and 40 minutes.

4.2.4 Adding measured data from fieldwork

To finally make a realistic model of the actual temperature distribution in the snowpack observed in Sogndalsdalen, we included data from our fieldwork. The earlier models only showed how and when lack of surface hoar growth would give lower temperatures in a snowpack, compared to a snowpack with surface hoar growth. In this section we have explored how much surface hoar affects the temperature gradient compared to the other terms of the energy balance equation (EQ. 1). In order to add real data from field, the model was extended to the full depth (44 cm) of the snowpack at Hollekvebrui. However, density, effective conductivity, and specific heat capacity remained the same as in table 1 to not apply to many changes to the model at once. The initial condition was chosen as the temperature measurements from 18th of March. The depth segments Δx and time segments Δt were changed to have a more detailed resolution of 0.01 m and 75 s, respectively. We modelled the temperature change for 12 hours and 50 minutes, the time interval between measurements in field. The values used in the model with real data is listed in table 2.

Table 2: Values chosen for the model with real data.

Description	Values	
Density of snow, ρ_s	200	kg/m^3
Effective thermal conductivity, k_{eff} (W/m K)	0,1	W/(m*K)
Specific heat capacity snow, C_P	2090	J/kg K
Thickness of snowpack	0,44	m
Temperature at snow/ground interface (lower BC)	-0	°C
Total time (12 hours 50 min) t_{tot}	46200	s
Surface hoar created	0,094	kg/m^2
Depth intervals, Δx	0,01	m
Time intervals, Δt	75	s

Net radiation

Firstly, we investigated what effect only radiational energy (Q_N) would have on the temperature in the snowpack. In the model, the heat flux provided from the net radiation (q_{LW}) is the net longwave radiation measured from the weather station. The net shortwave radiation is presumed to be 0 W/m^2 as the sun will have set during the time of the experiment. The measured net shortwave radiation was low, but the values are assumed to be noise. The Neumann boundary equation (EQ. 21) was used, where:

$$\nabla u = -\frac{q_{LW}}{k} \tag{29}$$

Our measurements of longwave radiation were taken every 10 minutes, but as our model has a time interval of 75 seconds, we have extended the measured radiation heat flux for 600 seconds (10 minutes) (figure 22). This assumption seems reliable as the measured values (figure 13) have a low dispersion. The modelled temperature is shown in figure 21.

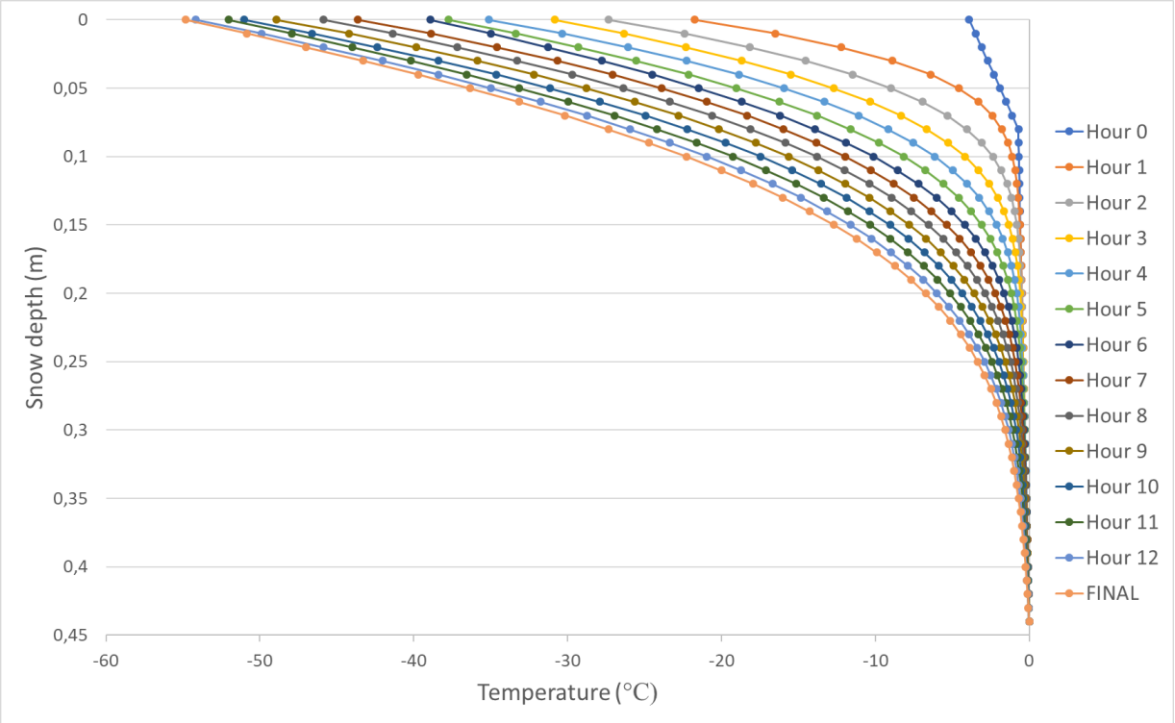

Figure 21: Hourly temperature change in the modelled snowpack. Only net radiation is used as heat flux in the upper boundary condition.

We are confident that the longwave radiation measured are somewhat correct, as we have compared them to radiation measurements provided by the Norwegian Water Resources and Energy Directorate (NVE) from the closest snow data stations, Vetlebotn and Kyrkjestølane, which are located at Voss and Filefjell, respectively. For the night of 18th to 19th of March the radiation fluxes vary between -38 and -75 W/m^2 at Vetlebotn and between -30 and -75 W/m^2 at Kyrkjestølane, while our measurements vary between -33 and -65 W/m^2.

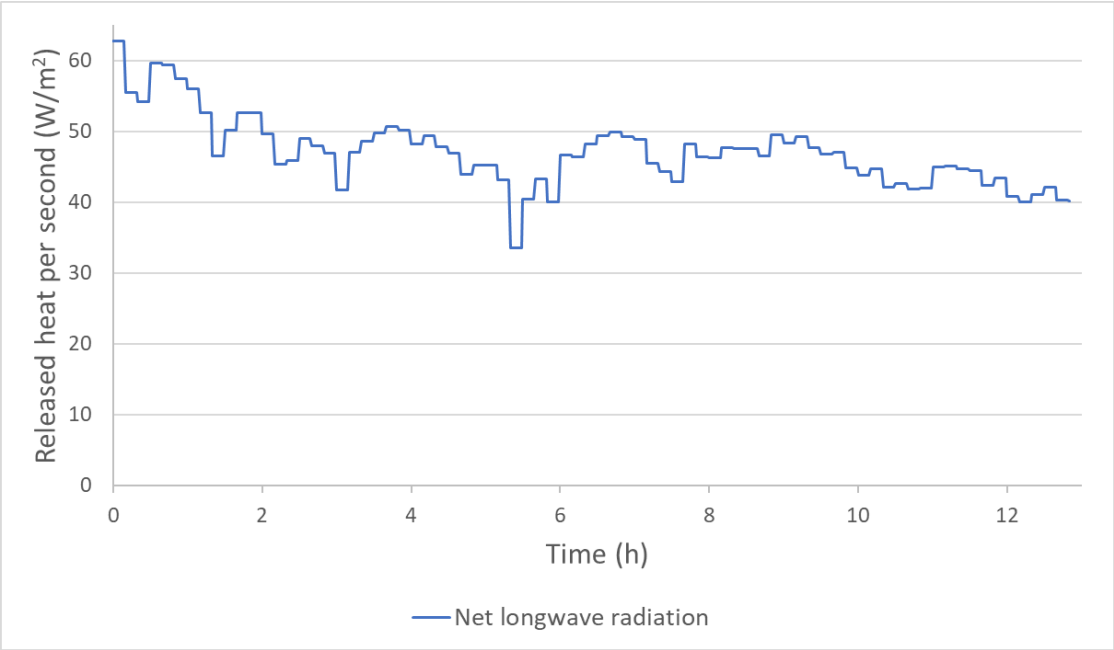

Figure 22: Released heat per second from net longwave radiation measured from the weather station. Positive values indicate outgoing fluxes. Every measured value is taken as an average for the 10 following minutes.

An aspect about the outgoing heat flux with only longwave radiation, is how the temperature gradient changes with time and depth (Figure 23). The 0 – 1 cm line is varying a lot with time, compared to the lines at lower depths. Because of the proximity to the snow surface, the snow at 0 – 1 cm quickly reacts to the variation in heat fluxes, and there is a lot of variation in the temperature gradient (figure 23). The relatively low effective conductivity of snow dampens this effect further down. The threshold value of 200°C/m is talked about in section 2.2. This is a high value for temperature gradients in a snowpack, meaning that it is reasonable to believe that growth of faceted crystals also would happen at lower temperature gradients. However, this threshold value makes it easier to compare how the temperature gradient changes with different input values.

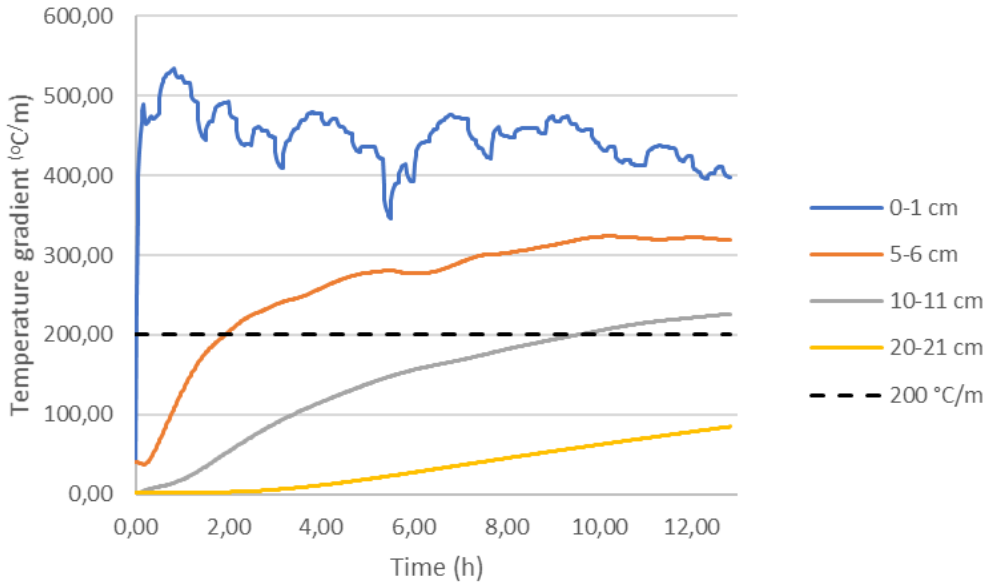

Figure 23: Temperature gradient plotted over time when only net radiation is included in the upper boundary condition. Each line represents a different depth showing the temperature gradient development with time. The temperature gradient of 200 °C/m is known to produce faceting over a short period of time.

The output surface temperatures from the model with only net radiation as outgoing heat flux are unrealistically low, as the temperature is as low as -54.82°C. The temperature gradients between 0 – 1 cm are over twice as high as our threshold value of 200°C/m. Considering this result, it is reasonable to assume that there must be a factor that counteracts to the outgoing longwave radiation. A possible supposition is that this heating comes from the latent heat release by surface hoar formation. To check if surface hoar growth is enough to change the temperature gradients to more similar results observed in field, the latent heat released is added to the boundary condition. This model is shown in the next section.

Latent heat

Using the approach described in section 4.2.1. the heat that is added to the snow through deposition of surface hoar was included in the simulation. This is the Q_e term of the surface energy balance equation (EQ. 1). A possible relationship between surface hoar growth and temperature difference between the air and the surface was mentioned in the section of linear heat release. However, due to our lack of instrumentation measuring the growth rate, we have chosen to use a constant latent heat release. There are several factors that affect the surface hoar formation, which vary throughout the night. These factors include relative humidity, wind speed, air temperature and surface temperature of the snow. Surface temperature is directly dependent on the surface hoar growth itself. With increased growth of surface hoar (increasing Q_e) the change in surface temperature will decrease, and thus the cooling of the air right above

the surface will slow down. Hachikubo (2001) has found that an increased roughness because of surface hoar growth gives an increased turbulence in the air. This results in a positive feedback effect on the vapor flux where the turbulence brings more water vapor down to the surface and contributes to further growth (Hachikubo, 2001). Possibly, this increased turbulence could also result in an increase in sensible heat, which could have a destructive effect on the surface hoar growth. However, this contributing factor is not emphasized in literature, which leads to the conclusion that larger surface hoar crystals will primarily result in an increased growth. Because of the uncertainty related to the rate of surface hoar growth, a constant latent heat release has been used.

To find the amount of surface hoar that can offset the unrealistically low temperatures found when only outgoing radiation is considered, different masses of surface hoar were used in the calculation of Q_e. The found mass of surface hoar that gave the right temperatures after 12 hours and 50 minutes was 0.525 kg, and thus the calculated heat flux was 32.56 W/m^2.

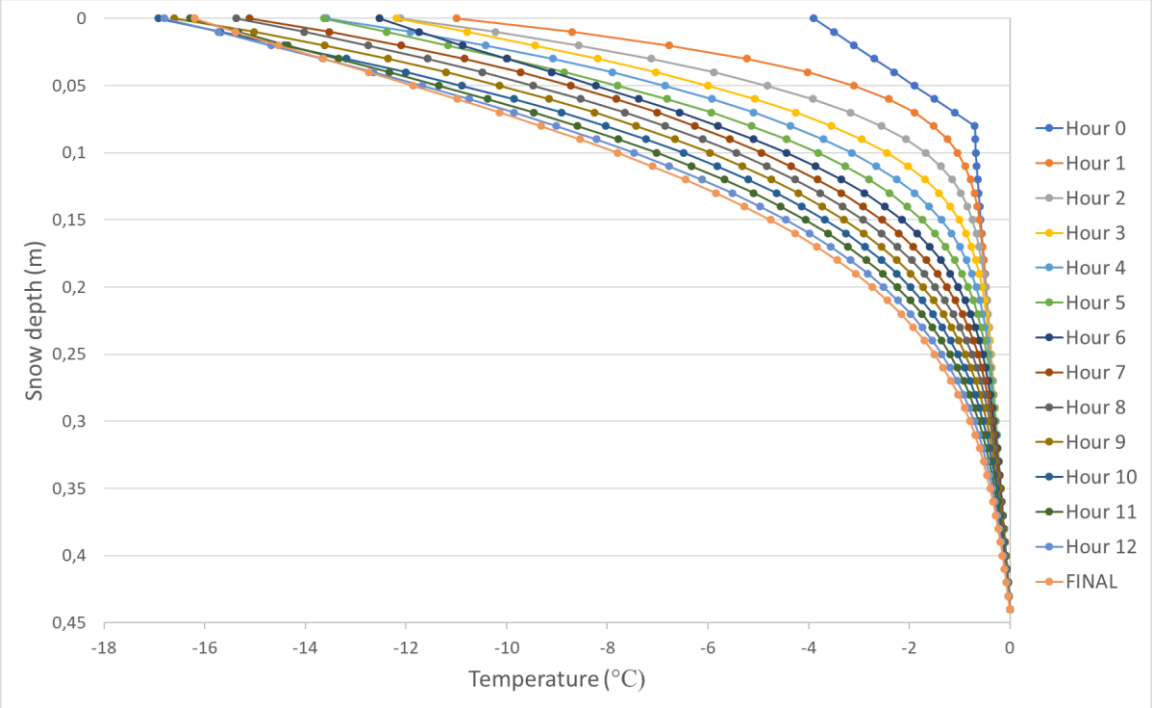

Figure 24: Hourly temperature change in the modelled snowpack. Net radiation and surface hoar growth of 0.525 kg. Final surface temperature (-16.2°C) is close to the measured temperature in figure 12.

The resulting temperature profile (figure 24) shows values closer to our measurements, with the lowest surface temperatures (-17.12°C) at 9 hours and 50 minutes. The final temperature was -16.2°C, meaning that the surface temperature has warmed the last two hours. A correlation between the heat fluxes can be seen in figure 25, which shows the outgoing heat flux when 0.525 kg of surface hoar is created and when no surface hoar is created. The resulting

temperature gradients with surface hoar are shown in figure 26. These are considerably lower compared to the gradients modelled without surface hoar (figure 23).

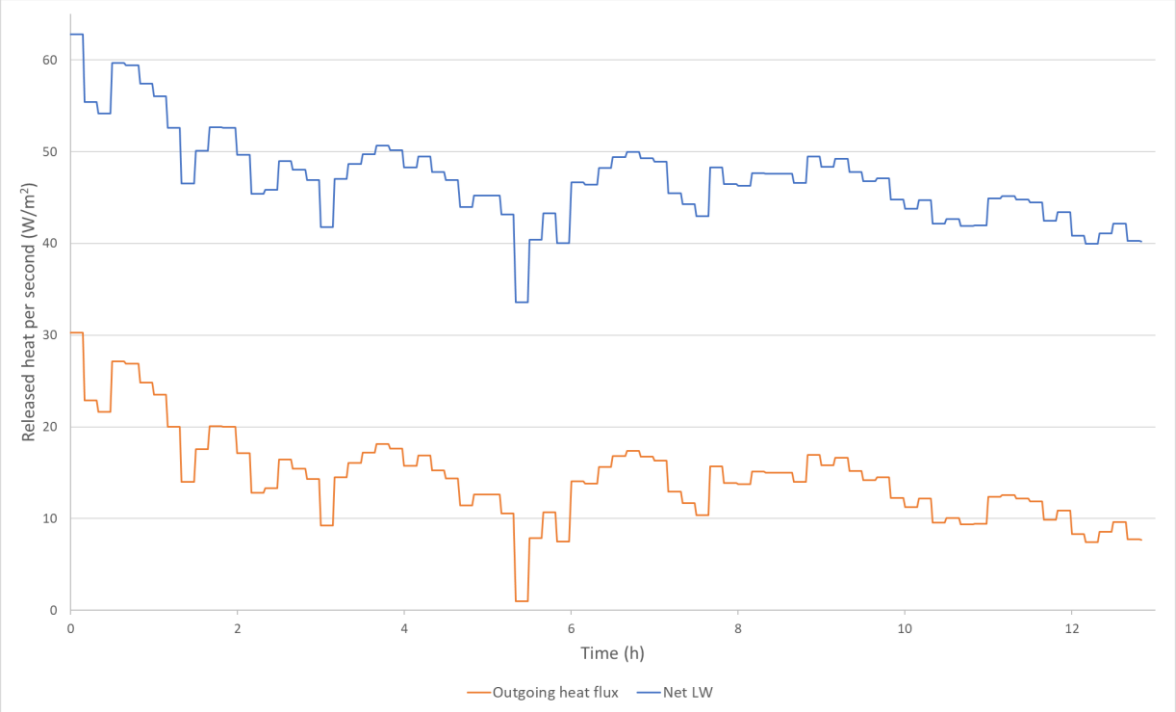

Figure 25: Outgoing heat flux from net long wave radiation (blue), and from net long wave radiation with constant heat flux from latent heat (0.525 kg of surface hoar) (orange). The total heat flux with radiation and latent heat (orange) is significantly smaller than heat flux form radiation (blue).

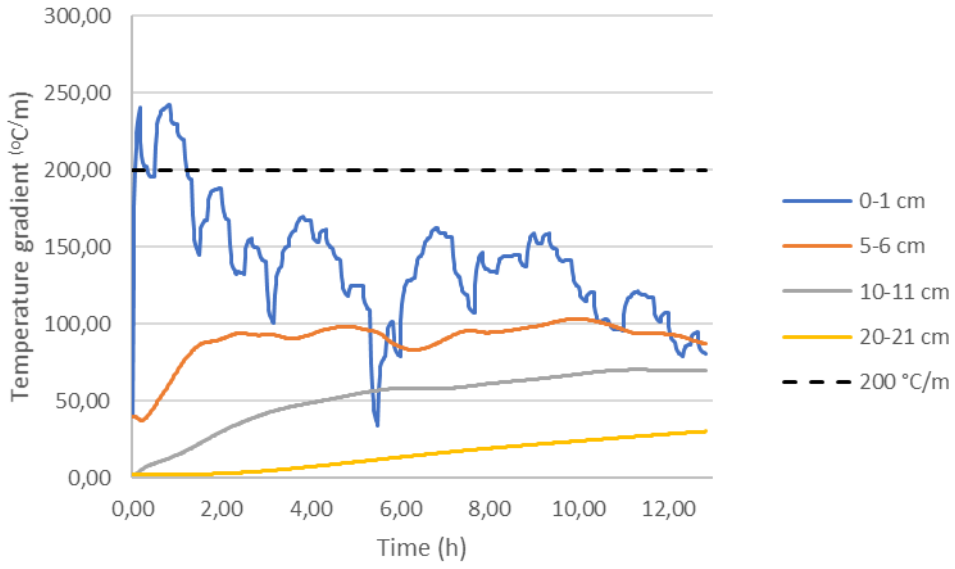

Figure 26: Temperature gradient of model with net radiation and latent heat from 0.525 kg of surface hoar plotted over time (12 hours 50 min). Each line represents a different depth showing the temperature gradient at the time.

The amount of surface hoar needed (0.525 kg) was considerably larger than we measured (0.094 kg), and what has been measured by both Stössel et al (2010) and Hachikubo & Akitaya (1997)

during their extensive studies. In an extreme case, a water source that contains warmer water, e.g. from hot springs, would produce vast amounts of water vapor. Given a cold enough snow surface, this could result in large amounts of surface hoar, possibly close to 0,5kg. However, these cases seldom occur at places with similar conditions as Hollekvebrui. 0.525 kg of surface hoar converts to a total latent heat of 1 504 650 J, in comparison to 269 404 J for 0.094 kg, which is 5.58 times more. The contributing factor of the latent heat flux (5.83 W/m^2 when 0.094 kg is used) is very small compared to the outgoing radiation flux (-33 – -65 W/m^2). To fully understand how surface hoar affects the snowpack the full energy balance equation must be included in the model. From several surface energy balance calculations (Holmgren, 1971; Marks & Dozier, 1992) we know that sensible heat will have a larger contribution, and this is the next term we tried to model.

Calculating sensible heat

As mentioned in section 3.2.1., sensible heat is difficult to calculate. For our measurements the most problematic factor to calculate proved to be the Bulk Richardson number (R_B). Oke (1995) writes that beyond values of 0.25 (to the left in figure 11) negative buoyancy dampens forced convection i.e. turbulent forces, and flows are nearly laminar. Because surface hoar has been observed, forced convection and inversion in the air above the snow surface has taken place. We also know that the flow has not been laminar due to the requirement of turbulent exchange for surface hoar growth (Colbeck, 1988). Thus, we know that our R_B-value should lie between 0 and 0.25. Hachikubo & Akitaya (1997) used a value between 0 and 0.2. Using equation 5 we have calculated our Bulk Richardson Number to be up to 0.339, which is not in the right range. When calculating the R_B values with data from Hachikubo & Akitaya (1997) at 0.1m and 1m, we notice that the R_B value differs with height. Different z values showed that R_B becomes smaller the closer to the ground the measurements are taken. At 1m R_B was 0.066, and at 0.1m at the same time interval R_B was 0.014. Considering our measuring height z is much larger (2.75 m) this could explain why our Bulk Richardson number becomes consistently larger than the limits of 0 – 0.2. Previous findings on similar calculations have also found that using measurements that are taken above 1m can produce significant errors to the results (Casinère, 1974; Halberstam & Schieldge, 1981).

While not ideal, assuming a constant value for the R_B term of the sensible heat is viable for seeing if the surface hoar formation will affect the temperature gradient in the snowpack. In the measurements from Hachikubo & Akitaya (1997), R_B varies between approximately 0.01 and

0.04, with most values around 0.01. We can use these values to assume a constant for R_B =0.015 for every time step and calculate the sensible heat from this. This allows for reasonable values of sensible heat that varies with winds speed and temperature difference. Hachikubo & Akitaya (1997) had continuous wind measurements that were averaged for 30 minutes. Since we only have 3 measurements for wind speed per 30 minutes, we use an average wind speed of 1.055 m/s (average of all measurements the night of 18th to 19th of March) in our calculations of sensible heat.

Since sensible heat is dependent on the surface temperature in the model, there is no reason to model only sensible heat alone. The sensible heat flux was modelled together with the radiative and latent heat fluxes, described in the next section.

4.2.5 Comparing computation with and without surface hoar

With radiative, sensible and latent heating, the upper boundary condition is calculated using equation 21. ∇u is calculated with equation 19 where q is calculated with:

$$q_{tot} = q_n + q_h + q_e \tag{30}$$

q_n is the radiative heat flux that is assumed to be only longwave radiation. q_h is the sensible heat flux calculated using equation 3, and q_e is the latent heat flux assumed only to be the heat flux related to the surface hoar growth, calculated using equation 24 where a mass of 0.094 kg of surface hoar was used. The resulting temperature gradient is seen in figure 27. The model was also run without surface hoar formed (Q_e= 0), with the resulting temperature gradients in figure 28. The two graphs do not differ a lot, but one of the distinctions can be seen in the graph of surface temperatures (figure 29). With modelled surface hoar growth, the surface temperatures after 12 hours and 50 minutes is -17.88 °C. Without surface hoar, the surface temperature after 12 hours and 50 minutes is -19.26 °C.

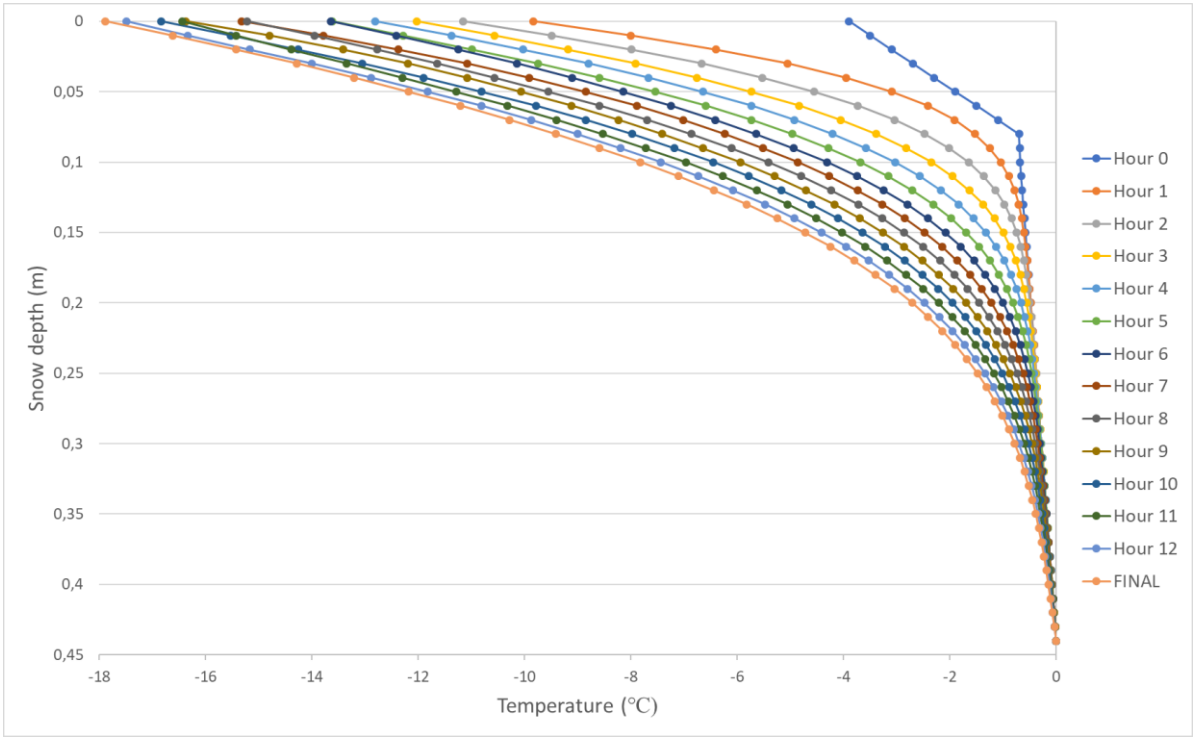

Figure 27: Hourly temperature change in the modelled snowpack. Heat flux is dependent on latent heat, sensible heat and outgoing longwave radiation.

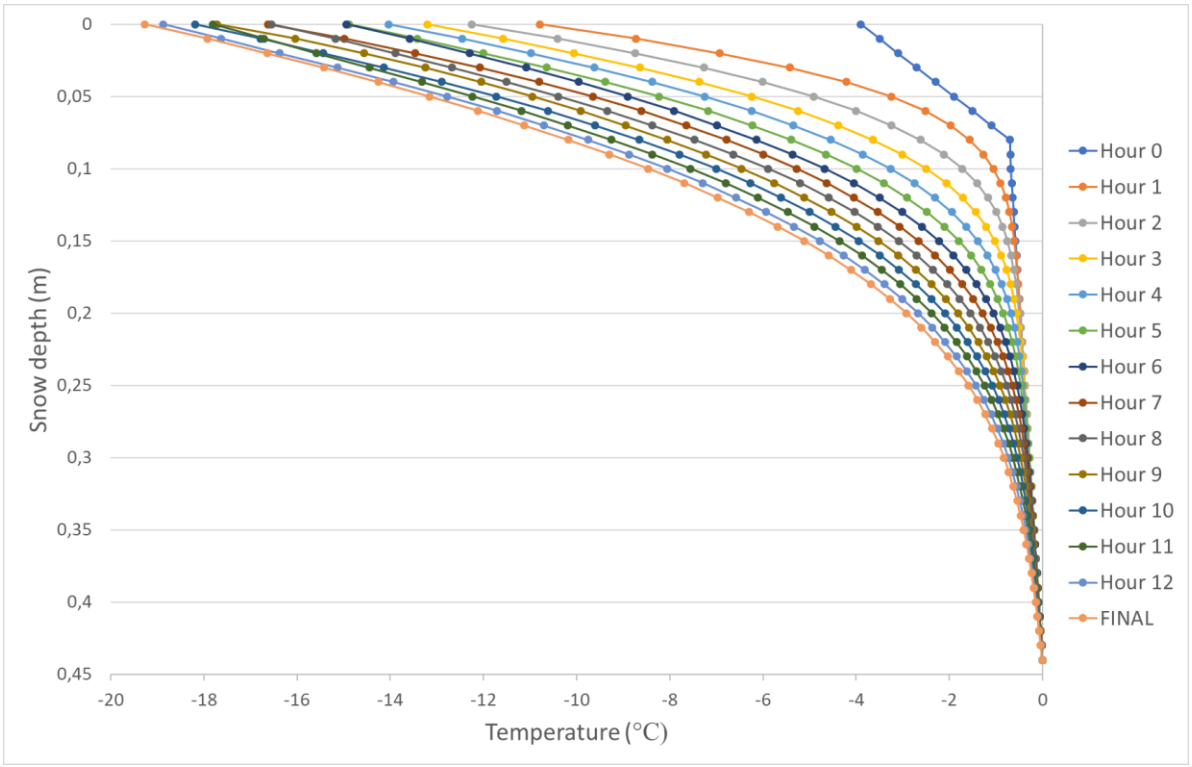

Figure 28: Hourly temperature change in the modelled snowpack. Heat flux is dependent on sensible heat and outgoing longwave radiation.

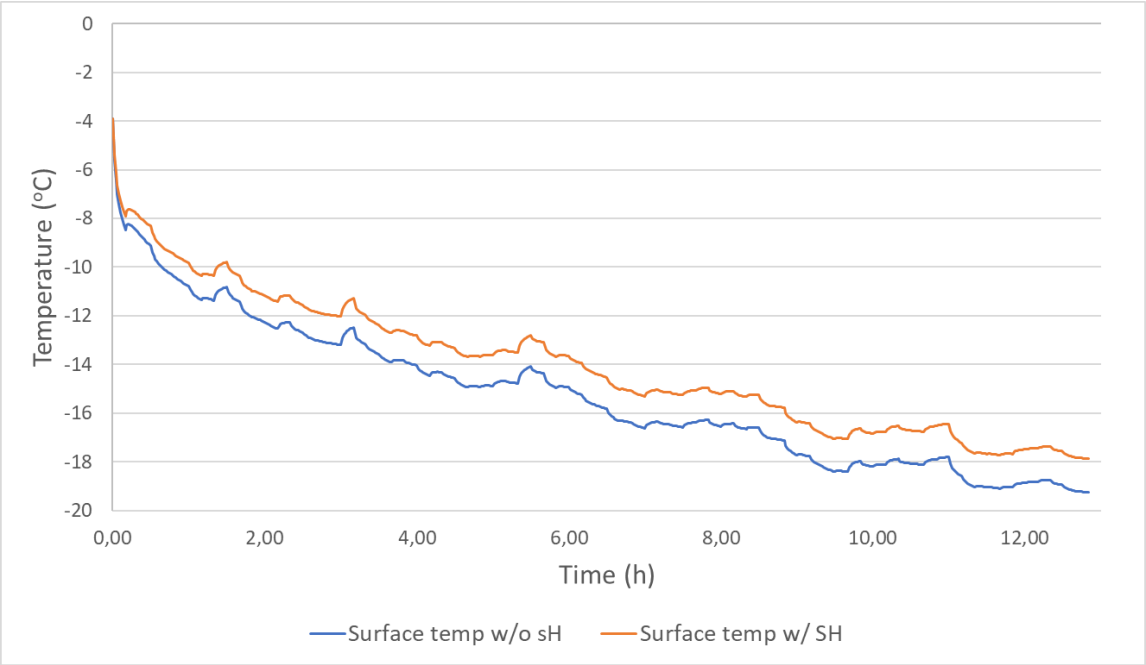

Figure 29: Difference in surface temperature with and without surface hoar growth on the surface. With sensible heat and radiation.

When all elements in equation 30 are applied, the temperature gradient shows that for most of the night the temperature gradient at the surface is lower than 200°C/m (figure 30**a**). When surface hoar is not formed ($Q_e = 0$), the temperature gradient is a little higher in the earlier hours of the night at the same depths (figure 30**b**). Towards the end of the night the temperature gradients are very similar both with and without surface hoar formation.

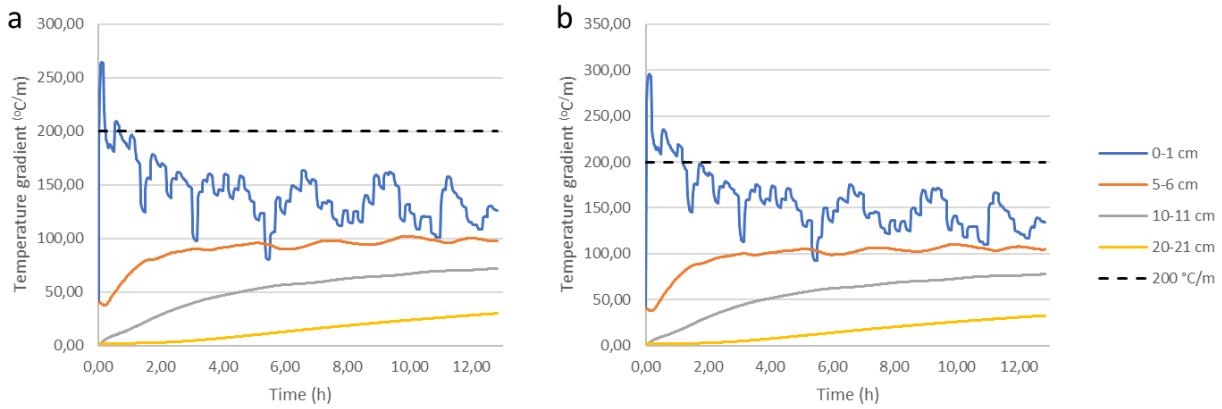

Figure 30: Temperature gradient plotted over time. Each line represents a different depth showing the temperature gradient at the time. Figure **a** shows the temperature gradient with surface hoar formation and **b** shows the temperature without surface hoar formation

The released heat is higher in the earlier hours and decreases slowly with time. In the first ten minutes the released heat is very large, which shows the reason the surface temperature

decreases so fast at the same time (figure 29). The released heat varies in the same pattern as the outgoing longwave radiation showed in figure 22. However, it curves slightly where the longwave radiation was flat, as seen in figure 31. This is due to the sensible heat that changes in every time step whereas the longwave radiation stays constant for 10 minutes. The difference in the released heat modelled with and without surface hoar is decreasing as time passes and is almost equal after 12 hours 50 min. The sudden decreasing values at around 1.5 hours, 3 hours and 5.5 hours (figure 31) correspond with the surface temperature increases seen in figure 29. The same goes for the period at 9-11 hours which also has a slight surface temperature increase.

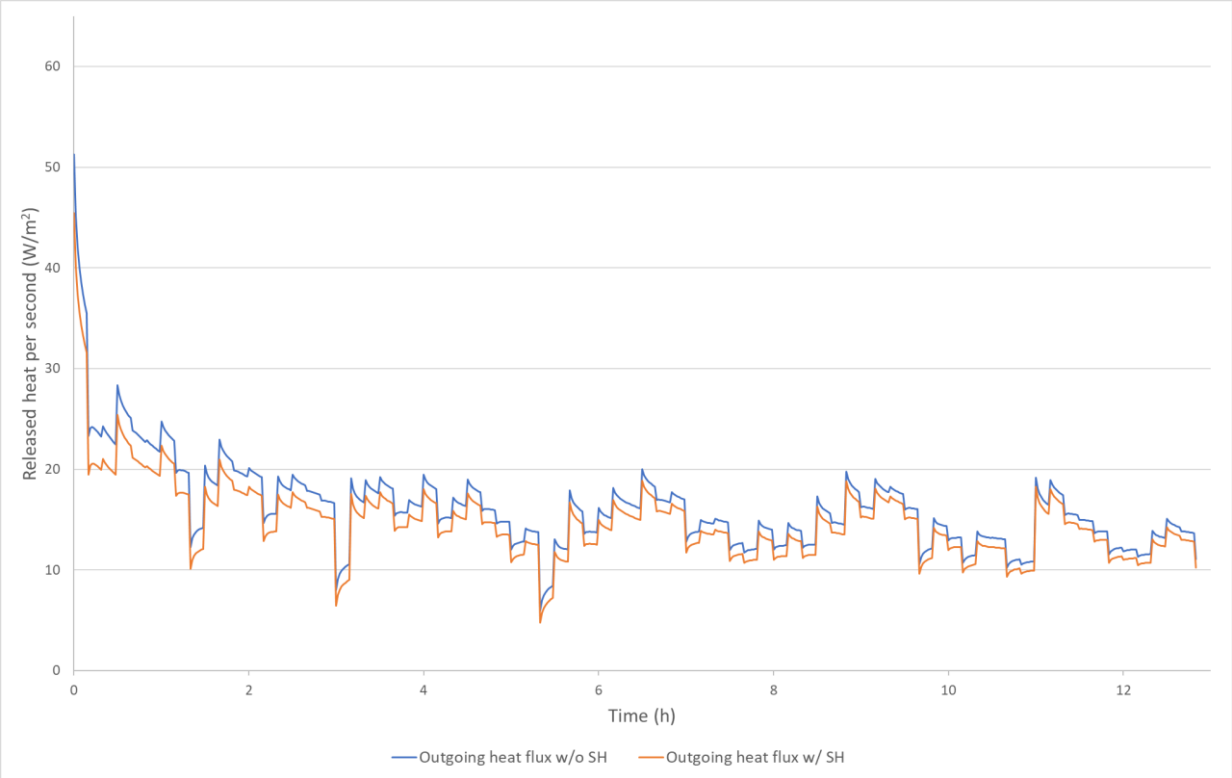

Figure 31: Graphs showing how the outgoing heat from the snowpack changes with time. The orange line shows how much heat is released when surface hoar is formed, while the blue line shows how much heat is released when surface hoar is not formed.

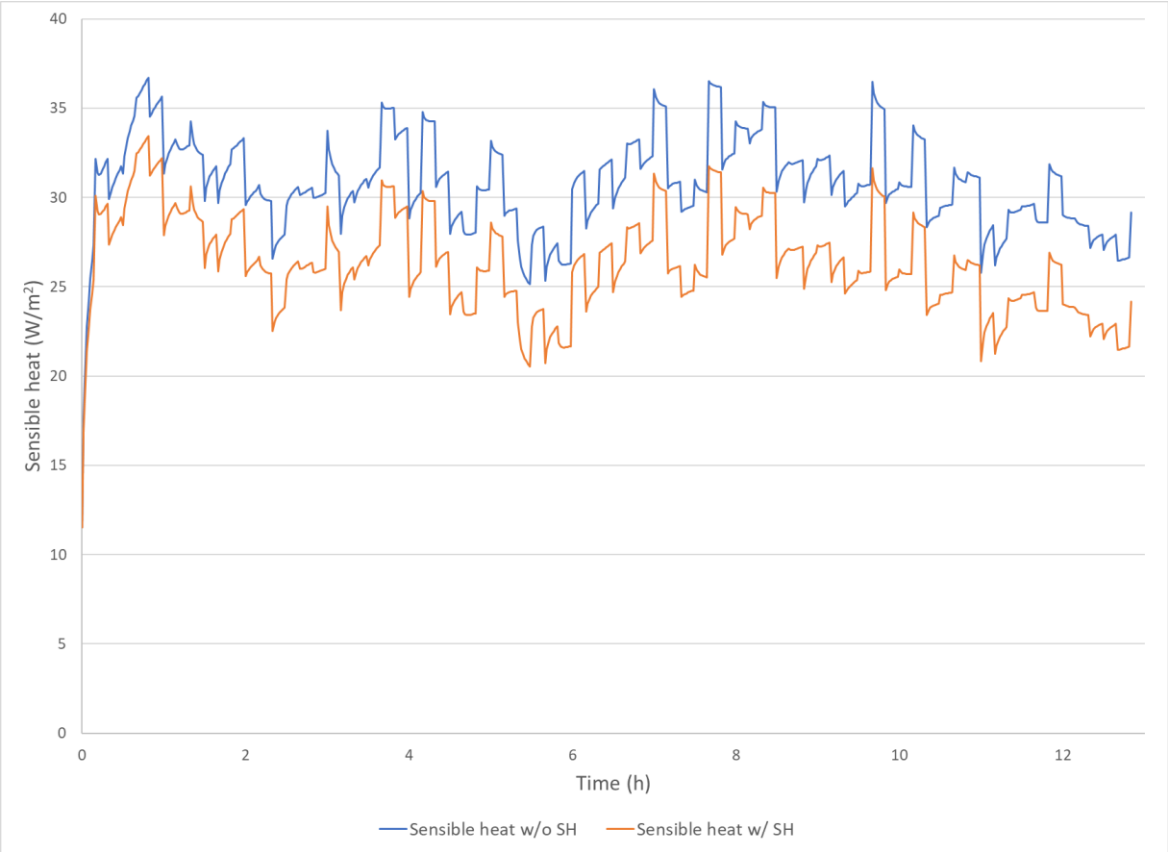

Figure 32: Sensible heat modelled with and without surface hoar. The difference is increasing with time and equivalates the surface hoar growth at the end of the computation (12 hours 50 minutes).

Setting the q_e (latent heat flux) term of equation 30 to 0 W/m^2 the temperature gradients plotted at every hour do not change significantly (figure 27 and 28). The heat flux from the top is plotted in figure 31 and even with constant heat released from surface hoar growth the difference between the two graphs decreases with time. The fact that the sensible heat is dependent on the surface temperature in the snowpack proves problematic. When the heat flux from surface hoar is removed, the sensible heat increases almost to the same level as the heat flux from surface hoar growth (figure 32). This is because the sensible heat is dependent on the surface temperature, which additionally decreases when latent heat is removed, which again increases the sensible heat. This explains how the difference in total heat flux becomes smaller in figure 31.

We notice several problems with the model after we have added all the factors that we can measure. During the first ten minutes the surface layer cools from -3.9°C to -7.9°C. This leads us to assume something is not correct with our input information. Because the measurements from field are limited for the initial temperature, it is possible that the initial condition is what is causing the problem. The initial temperature may have a very different curve between the

three known points. The issue with rapid cooling shows how the model contains large issues that must be asserted before making final conclusions.

At several time intervals during the night the snow will become warmer, which can prove problematic as the sensible heat is always lower than the net longwave radiation. This means that the ground and surface hoar formation is heating the snowpack up. This is possibly not a real issue with the model and may be the reality for the snow surface, but looking at figure 33 which zooms in on the issue it seems that the times the surface heats up, the cooling is increased. The heating is caused by fluctuations in longwave radiation and when the heating happens, sensible heat goes down and the surface is effectively cooled more. Without additional measurements we cannot confirm this surface temperature increase.

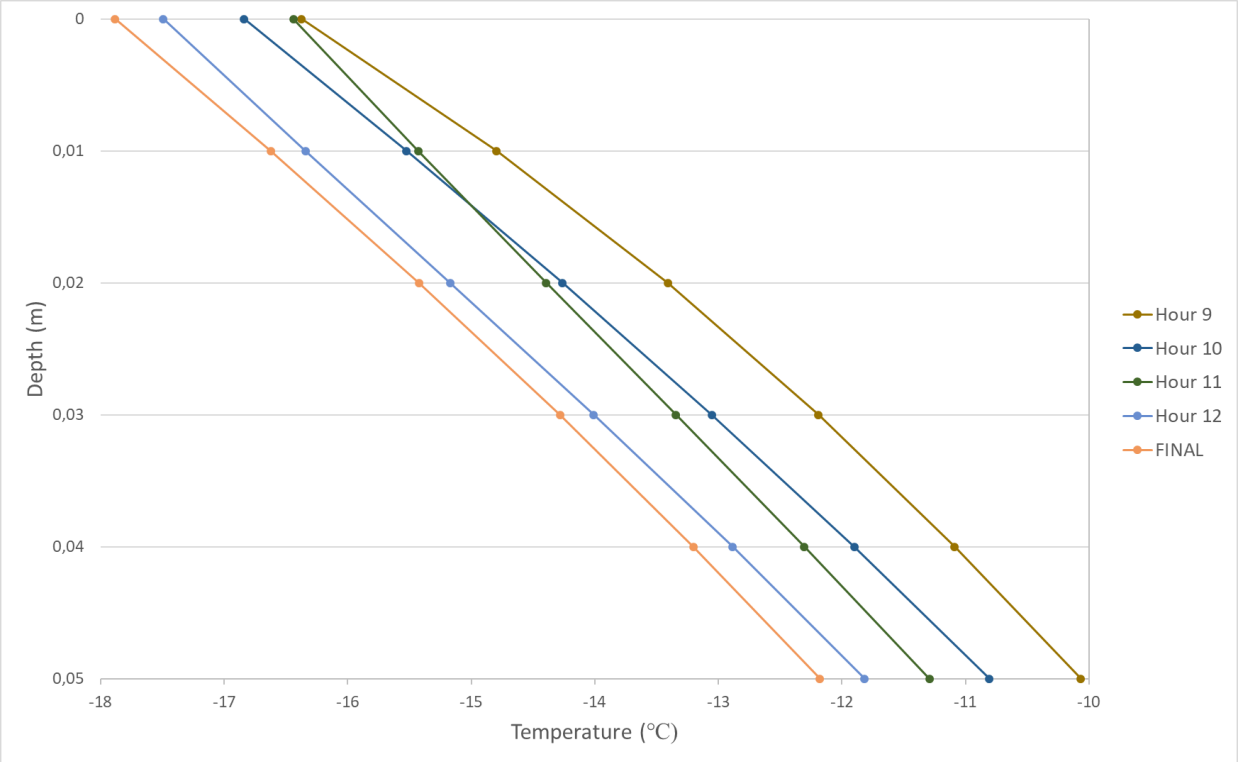

Figure 33: Temperature graphs from the last four hours. The surface temperature at hour 11 (green line) is warmer than at hour 10 (dark blue line).

4.2.6 Vapor pressure gradient

The process of creating near surface faceted crystals is dependent on vapor pressure gradients, as explained in 2.2. So far, temperature gradients have been investigated, which only indirectly shows the effect. To see if surface hoar affects the faceting process, we have converted temperatures to vapor pressure, using equation 23. The vapor pressures calculated for each temperature in the model are shown in figure 34 and 35, where figure 34 is modelled with surface hoar formation and figure 35 is without surface hoar. No substantial difference is

observed between the two graphs. The vapor pressure decreases with time but not at the same rate as the temperature decreases (figure 27 and 28). This confirms the non-linear relationship between temperature gradients and vapor pressure gradient (figure 4).

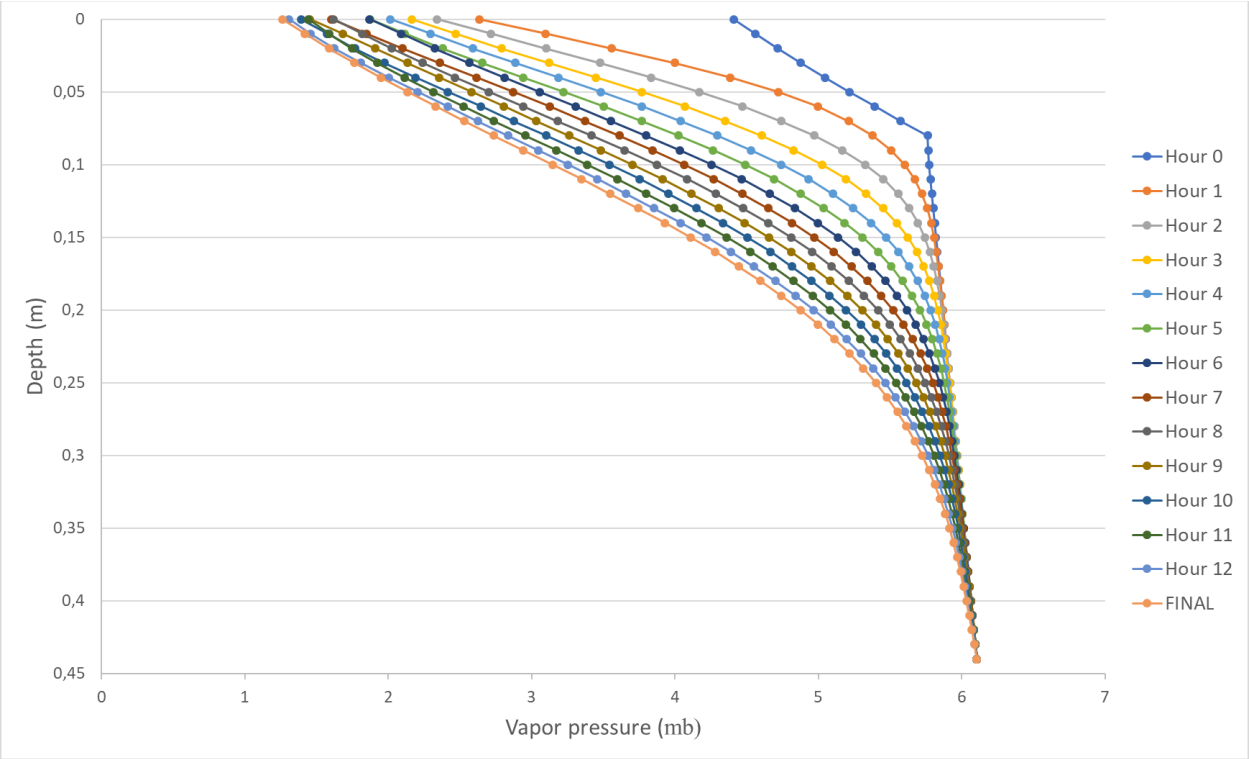

Figure 34: Plotted hourly vapor pressure. Graph is modelled with surface hoar.

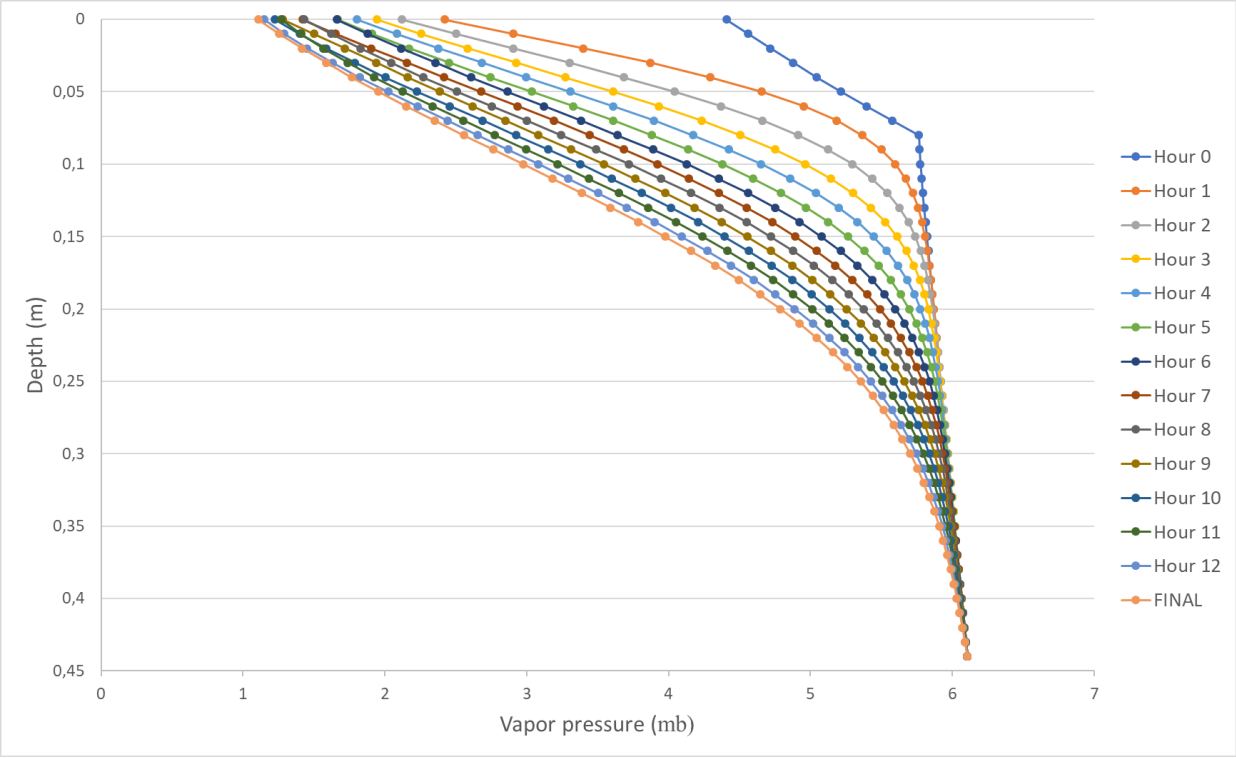

Figure 35: Plotted hourly vapor pressure at different depths. Graph is modelled without surface hoar.

The vapor pressure gradients at different depths, with and without surface hoar, are shown in figure 36. The dotted line at 25mb/m in both **a** and **b** can be used as a reference to see how long the gradients stays above this value, which is talked about in section 2.2. The vapor pressure gradients without surface hoar (figure 36b) are slightly higher in the beginning but decreases rapidly and ends up being below the threshold value at approximately the same time as the gradients with surface hoar (figure 36a), meaning they are above the threshold value for almost the same amount of time. The model without surface hoar has values above 25 mb/m for 41 minutes longer than the model with surface hoar. The 0 – 1cm line is varying a lot with time, compared to the lines at lower depths. Further we see that the vapor pressure gradient is higher at 5 – 6cm depth than at 0 – 1cm from hour 5 until the end of the modelling. The gradient at depth 10 – 11cm also becomes larger than at the surface but only after 7 hours, and is almost equal to the gradient at 5 – 6cm.

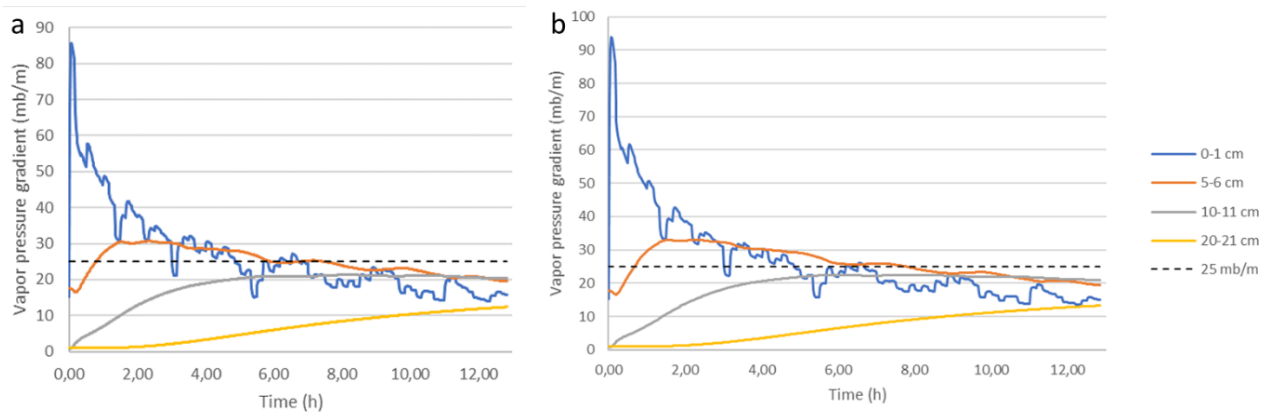

Figure 36: Vapor pressure gradients at different depths plotted with time. **a** shows the vapor pressure gradient with surface hoar formation and **b** shows the vapor pressure gradient without surface hoar formation.

4.3 Improvements on field method and further development of the model

Ideally, the field measurements would have been conducted at minimum two different study locations. Temperature measurements from both a location close to a water source and a location without a water source would possibly make it easier to observe if the creation of surface hoar affects the temperature gradient in the snowpack. Also, to further compare and get better results it could have been necessary to continuously monitor the temperature gradient in the snowpack throughout clear nights. More detailed measurements of the sensible heat are highly recommended. Both higher resolutions, more frequent measurements continuously throughout the night, and measurements at lower elevation would increase the accuracy of the

sensible heat calculations in the model. This would show how the surface hoar growth will have affected the temperature gradient, giving comparable data.

As seen in figure 12, the snowpack at Hollekvebrui consisted of four separate snow layers, which we have added in the model with different conductivities and densities (Appendix IV). Since only layer hardness and grain type was registered in the field, the conversion chart made by Jamieson & Schweizer (2000) were used to find the densities, and suitable effective conductivities were found from Sturm and Johnson's graph (figure 3). The final surface temperature (with 0.094 kg of surface hoar) reached -18.5°C, which is almost the same as the model without layering. Due to the little difference, we have chosen not to present the resulting graphs from the model with layering. However, in cases where the snow has very different conductivities within the upper 10 cm, the layers should definitely be modeled. Our model with layering is attached in Appendix VI. We also made a model where we increased the resolution by setting Δx to 0.001 m. Δt was set to 1 second to accommodate for equation 22. This did not change the result other than increasing the computing time.

The problem with the rapidly decreasing temperature the first 10 minutes was probably due to a poorly defined initial condition in section 4.2.5. A simple way to eliminate the problem might be to run several cycles of a full 24-hour simulation, including an internal heating term that decreases with depth, representing the incoming shortwave radiation during the day. This iterative process could be a good way of calibrating the parameterization of the model.

5. Conclusion

In this bachelor thesis we have developed a numerical model of the temperature in the snowpack, using input values from field work in Sogndalsdalen. Through a step-by-step process the model was gradually developed. The last model was computed twice: once with formation of surface hoar and once without. With surface hoar the final surface temperature was -17.88°C, and without surface hoar the final temperature was -19.26°C. Both the models reached temperature gradients above 200°C/m, however the model without surface hoar showed slightly larger values. Based on the data found in our model, surface hoar formation does not seem to have a large effect on the surface temperature of snow. The vapor pressure gradients were also calculated and shows that the model without surface hoar has values over 25 mb/m for 41 minutes longer than the model with surface hoar. At times we observed that the vapor pressure gradient at the surface was lower than the vapor pressure gradient further down in the snowpack (at 5-6 cm and 10-11 cm). This shows how faceting processes could continue further down in the snowpack while the surface is warming.

However, there were several sources of error that disprove/invalidates the result of our model. Firstly, some of the values used in the model are based on one single field day in March of 2019. In addition, we are not confident that the temperature gradients modelled are correct. Sampling through one or two entire winter seasons would provide more data to get a better understanding of the dynamics of the temperature in a given snowpack. An additional study site at a location without proximity to a water source would allow us to compare snowpacks with and without surface hoar growth. However, due to time restrains and a season with poor conditions for surface hoar formation, we have not been able to gather a significant amount of data. We would therefore need to extend the dataset to test the findings of this study.

6. References

Anderson, E. A. (1976). *A point energy and mass balance model of a snow cover*. Retrieved from Silverspring, Md:

Armstrong, R. L. (1985). *Metamorphism in a subfreezing, seasonal snow cover: The role of thermal and vapor pressure conditions.* (Ph.D), University of Colorado, Colorado.

Armstrong, R. L., & Brun, E. (2008). *Snow and Climate: Physical Processes, Surface Energy Exchange and Modeling*: Cambridge University Press.

Birkeland, K. W. (1998). Terminology and Predominant Processes Associated with the Formation of Weak Layers of Near Surface Faceted Crystals in the Mountain Snowpack. *Arctic and Alpine Research, 30*, 193-199. doi:10.1080/00040851.1998.12002891

Birkeland, K. W., Johnson, R. F., & Schmidt, D. S. (1998). Near Surface Faceted Crystals Formed by Diurnal Recrystallization A Case Study of Weak Layer Formation in the Mountain Snowpack and its Contribution. *Arctic and Alpine Research, 30*, 200-204. doi:10.1080/00040851.1998.12002892

Brandt, R. E., & Warren, S. G. (1993). Solar-heating rates and temperature profiles in Antarctic snow and ice. *Journal of Glaciology, 39*(131), 99-110.

Casinère, A. C. d. L. (1974). Heat exchange over a melting snow surface. *Journal of Glaciology, 13*(67), 55-72. doi:https://doi.org/10.3189/S0022143000023376

Colbeck, S. C. (1983). Theory of Metamorphism of Dry Snow. *Journal of Geophysical Research, 88*, 5475-5482. doi:https://doi.org/10.1029/JC088iC09p05475

Colbeck, S. C. (1988). On the Micrometeorology of Surface Hoar Growth on Snow in Mountainous Area. *Boundary-Layer Meteorology, 44*(1), 1-12. doi:https://doi.org/10.1007/BF00117290

Dozier, J., & Warren, S. G. (1982). Effect of viewing angle on the infrared brightness temperature of snow. *Water Resources Research, 18*(5), 1424-1434. doi:10.1029/WR018i005p01424

Gagne, G. (2013). Observation: Grizzly Gulch. In. Utah Avalanche Center.

Gray, D. M., & Male, D. H. (Eds.). (1981). Handbook of snow: principles, processes, management & use. Pergamon.

Hachikubo, A. (2001). Numerical modelling of sublimation on snow and comparison with field measurements. *32*(1), 27-32. doi:10.3189/172756401781819265

Hachikubo, A., & Akitaya, E. (1997). Effect of wind on surface hoar growth on snow. *Journal of Geophysical Research, 102*(D4), 4367-4373. doi:10.1029/96JD03456

Halberstam, I., & Schieldge, J. P. (1981). Anomalous Behavior of the Atmospheric Surface Layer over a Melting Snowpack. *20*(3), 255-265. doi:10.1175/1520-0450(1981)020<0255:Abotas>2.0.Co;2

Hock, R. (2005). Glacier melt: a review of processes and their modelling. *Progress in Physical Geography, 29*(3), 362–391.

Holmgren, B. (1971). *Climate and energy exchange on a sub-polar ice cap in summer : Arctic Institute of North America Devon Island Expedition 1961-1963.* (175), Almqvist & Wiksell distr., Uppsala, Stockholm.

Horton, S., & Jamieson, B. (2017). Spectral measurements of surface hoar crystals. *Journal of Glaciology, 63*(239), 477-486. doi:10.1017/jog.2017.6

Jamieson, B., & Schweizer, J. (2000). Texture and strength changes of buried surface-hoar layers with implications for dry snow-slab avalanche release. *Journal of Glaciology, 46*(152), 151-160. doi:https://doi.org/10.3189/172756500781833278

Jordan, R., O'Brien, H., & Albert, M. R. (1989). *Snow as a thermal background: preliminary results from the 1987 field test*. Retrieved from Hanover, NH:

Järvinen, O., & Leppäranta, M. (2013). Solar radiation transfer in the surface snow layer in Dronning Maud Land, Antarctica. *Polar Science, 7*(1), 1-17. doi:10.1016/j.polar.2013.03.002

LaChapelle, E. R., & Armstrong, R. L. (1977). *Temperature patterns in an alpine snow cover and their influence on snow metamorphism*. Retrieved from

Lang, R. M., Leo, B. R., & Brown, R. L. (1984). Observations on the growth process and strength characteristics of surface hoar. *Proceedings of the International Snow Science Workshop*, 188-195.

Marks, D., & Dozier, J. (1992). Climate and Energy Exchange at the Snow Surface in the Alpine Region of the Sierra Nevada, part 2. Snow Cover Energy Balance. *WATER RESOURCES RESEARC, 28*(11), 3043-3054.

McClung, D., & Schaerer, P. (2006). *The Avalanche Handbook* (C. U. Hosler & L. McGehee Eds. 3rd edition ed.). Seattle, WA: The Mountaineers Book.

Oke, T. R. (1995). *Boundary Layer Climates* (2. edition ed.): Methuen & Co. Ltd.

Sturm, M., & Johnson, J. B. (1992). Thermal Conductivity Measurements of Depth Hoar. *Journal of Geophysical Research, 97*, 2129-2139.

Stössel, F. (2007). *Surface Hoar Formation on the Snow Surface due to Interactions with the Atmospheric Surface Layer.* (Master of advanced studies (MAS) Master's Diploma Project), Swiss Federal Institute of Technology Zurich, Zurich. (78)

Stössel, F., Guala, M., Fierz, C., Manes, C., & Lehning, M. (2010). Micrometeorological and morphological observations of surface hoar dynamics on a mountain snow cover. *Water Resources Research, 46*, 11. doi:10.1029/2009wr008198

Sverdrup, H. U. (1935). The eddy conductivity of the air over a smooth snow field.

van As, D. (2011). Warming, glacier melt and surface energy budget from weather station observations in the Melville Bay region of northwest Greenland. *Journal of glasiology, 57*(202), 208-220.

Warren, S. G. (1982). Optical properties of snow. *Reviews of geophysics and space physics, 20*(1), 67-89.

7. List of Appendices

I Weather data AWS

Weather data from the automatic weather station near Hollekvebrui in Sogndalsdalen presented in an excel file

II Radiation data NVE

Radiative measurements from the snow data stations in Voss and Filefjell presented in an excel file

III Field days

A table of field days at Hollekvebrui including measured mass gain, temperature, and snow stratigraphy

IV Table 3 layers

A table of snow layering and corresponding properties used in model with layering

V Model with constant heat release

Simple model with constant heat release equal to surface hoar growth presented in an excel file

VI Model with layering

Model with full surface energy balance and layering presented in an excel file